Available online at www.sciencedirect.com
SCIENCE DIRECT®
Journal of Computational and Applied Mathematics 193 (2006) 413–436
JOURNAL OF COMPUTATIONAL AND APPLIED MATHEMATICS
www.elsevier.com/locate/cam

RCMS: Right Correction Magnus Series approach for oscillatory ODEs

Ilan Degani[a,*], Jeremy Schiff[b]

[a] *Department of Mathematics, Weizmann Institute of Science, Rehovot 76100, Israel*
[b] *Department of Mathematics, Bar-Ilan University, Ramat Gan 52900, Israel*

Received 29 October 2003; received in revised form 12 January 2005

Abstract

We consider RCMS, a method for integrating differential equations of the form $y' = [\lambda A + A_1(t)]y$ with highly oscillatory solution. It is shown analytically and numerically that RCMS can accurately integrate problems using stepsizes determined only by the characteristic scales of $A_1(t)$, typically much larger than the solution "wavelength". In fact, for a given t grid the error decays with, or is independent of, increasing solution oscillation. RCMS consists of two basic steps, a transformation which we call the right correction and solution of the right correction equation using a Magnus series. With suitable methods of approximating the highly oscillatory integrals appearing therein, RCMS has high order of accuracy with little computational work. Moreover, RCMS respects evolution on a Lie group. We illustrate with application to the 1D Schrödinger equation and to Frenet–Serret equations. The concept of right correction integral series schemes is suggested and right correction Neumann schemes are discussed. Asymptotic analysis for a large class of ODEs is included which gives certain numerical integrators converging to exact asymptotic behaviour.

Keywords: Oscillatory differential equations; Right correction; Magnus series; Neumann series; Long step integrator; Asymptotic analysis

1. Introduction and definition of RCMS

One of the long standing challenges in numerical analysis is integration of differential equations with highly oscillatory solution. We address a particular class of such equations and describe an approach giving numerical integrators whose performance benefits from the severe oscillation instead of suffering from it.

Consider the linear ODE

$$y' = [A(\lambda) + A_1(t)]y, \tag{1}$$

where for all t, λ the eigenvalues of $A(\lambda) + A_1(t)$ have zero real part and some grow in absolute value as $\lambda \to \infty$. Generally, the solution of (1) will become severely oscillatory (this does not exclude unbounded solutions) as $\lambda \to \infty$ and standard numerical integrators will have to advance in small steps.

* Corresponding author. Present address: Department of Chemical Physics, Weizmann Institute of Science, Rehovot 76100, Israel. Tel.: +972 8 9343723; fax: +972 8 9344123.
E-mail addresses: ilan.degani@weizmann.ac.il (I. Degani), schiff@math.biu.ac.il (J. Schiff).

0377-0427/$ - see front matter © 2005 Elsevier B.V. All rights reserved.
doi:10.1016/j.cam.2005.07.001

The approach suggested here is based on two principles, transformation to the right correction equation and approximation of its solution using an integral series. The idea of right correction, known in quantum mechanics as the "interaction representation" [27], is the following. Suppose we wish to solve the linear ODE $w' = (P + Q)w$ where P and Q are time dependent matrices. If the fundamental solution z of $z' = Pz$ is known we can write $w = zu$. u is called the *right correction* and must satisfy the basic *right correction equation* $u' = (z^{-1}Qz)u$. Restricting t to the nth grid interval, one choice of a constant approximation for $A(t)$ is $\bar{A}_1 = 1/(t_{n+1} - t_n) \int_{t_n}^{t_{n+1}} A_1(t)\,\mathrm{d}t$. Eq. (1) can be written

$$y' = [(A(\lambda) + \bar{A}_1) + (A_1(t) - \bar{A}_1)]y, \quad t \in [t_n, t_{n+1}]. \tag{2}$$

In each grid interval the right correction $u_n(t)$, $t \in [t_n, t_{n+1}]$, is defined by the equation $y(t) = \exp[(t - t_n)(A(\lambda) + \bar{A}_1)]u_n(t)$. u_n satisfies

$$u_n' = B_n(t)u_n, \quad t \in [t_n, t_{n+1}], \tag{3}$$

where

$$B_n(t) = \exp[-(t - t_n)(A(\lambda) + \bar{A}_1)](A_1(t) - \bar{A}_1)\ \exp[(t - t_n)(A(\lambda) + \bar{A}_1)].$$

For large λ the restrictions on the eigenvalues of $A(\lambda) + A_1(t)$ will generally cause the entries of $B_n(t)$ to be highly oscillatory as functions of t; moreover, the difference $(A_1(t) - \bar{A}_1)$ makes $\|B_n(t)\|$ small. Hence integral series representations of ODE solutions are ideal for (3). With suitable quadrature methods the severe oscillations in the integrands kill numerical errors and accelerate convergence. The small norm of the matrix in (3) is also favourable. Thus working with Eq. (3) and with an integral series representation of its solution is preferred over working with (1), where the coefficient matrix is non-oscillatory with large norm. Our numerical implementation uses the Magnus series giving a Lie group integrator. The Neumann series, which avoids use of the matrix exponential but does not respect Lie group structure, is another possibility which may be suitable for large systems. The Right Correction Magnus Series (RCMS) integrators constructed along these lines are highly accurate and very efficient when compared to standard integrators applied to Eq. (1).

We must mention that in some cases, which are avoided in this work, $\|B_n(t)\|$ may be an unbounded function of t for fixed λ. This can happen, for example, if $A(\lambda) + \bar{A}_1$ is not diagonalizable or if we drop the assumption that the eigenvalues of $A(\lambda) + A_1(t)$ have zero real part. Even so the properties of the right correction integral series approach may still exert their positive influence, as discussed in [7,6]. It is also explained in these references why the right correction is prefered over the left correction.

In [9] Iserles has presented the "modified Magnus method". This method and RCMS, which were conceived and developed independently,[1] use the same basic approach, application of a Magnus series integrator to the right correction equation. The discussion in [9] centres on 2×2 "linear oscillator" equations and the problem of quadrature is avoided by applying the modified Magnus method only to problems allowing analytic integration in the right correction Magnus series, e.g. the Airy equation. In [10,13], Iserles and Nørsett continue this line of work by addressing the essential problem of efficient quadrature, in case $A_1(t)$ has general entries, of the highly oscillatory integrals which appear in the right correction Magnus series. Other authors have also addressed integration of similiar highly oscillatory ODEs. In [17,18] Lubich and Jahnke have constructed highly efficient integrators for near adiabatic propagation in quantum mechanics. In [15] Ixaru et al. presented an exceptional shooting "eigensolver" for the 1D time independent Schrödinger equation whose heart is an ODE integrator suitable (also) for reconstructing high energy, highly oscillatory, eigenfunctions. In both cases the integrators can be viewed as right correction Neumann series schemes. All these independent and recent appearances indicate that the right correction integral series approach has great potential for solving highly oscillatory differential equations.

We proceed to give a brief overview of this paper. In Section 2 the basics of Magnus and Neumann series are recounted. Then efficient, high order, quadrature methods for integrals with highly oscillatory integrands are discussed. The properties of different projection operators, which can give non-interpolating polynomial approximants, occupy a central part in our analysis. In Section 3 RCMS is applied to "type A" equations, an example of which are the perturbed constant coefficient Frenet–Serret equations. In Section 4 RCMS is applied to the 1D Schrödinger equation.

[1] Accounts of the initial stages of our work can be found in the research proposal [4] and in the progress report [5].

It is analytically and numerically shown that RCMS can have high order in h and that for fixed step size the error is either λ independent or decaying with λ, i.e. the error does not grow as the solution becomes more oscillatory. Our discussion is based on asymptotic expansions of Magnus series terms yielding detailed asymptotic analysis of exact solutions and of numerical errors. In Section 5 we discuss the implications of our averaging approximation $\bar{A}_1$ of $A_1(t)$ and show that it has an important role in asymptotic analysis and in construction of RCMS integrators with exact asymptotic behaviour. Several observations and directions for future research are given in the conclusion. The appendix includes formulas giving approximations of right correction Magnus series as functions of the parameter λ and step size h. More detailed presentations of this work appear in the PhD thesis [6], and in the technical report [7].

2. Integral series and highly oscillatory quadrature

Numerical integrators for differential equations can be based on integral series representations of the solution. These are very different from traditional integrators where solution derivatives determine the error.

The simplest integral series can be obtained by applying Picard iteration to obtain the fundamental solution of the matrix linear ODE

$$y' = A(t)y, \quad y(0) = E. \tag{4}$$

We obtain

$$y(t) = E + \int_0^t A(\tau)\,\mathrm{d}\tau + \int_0^t A(\tau)\int_0^\tau A(\tau_1)\,\mathrm{d}\tau_1\,\mathrm{d}\tau + \int_0^t A(\tau)\int_0^\tau A(\tau_1)\int_0^{\tau_1} A(\tau_2)\,\mathrm{d}\tau_2\,\mathrm{d}\tau_1\,\mathrm{d}\tau + \cdots \tag{5}$$

This series is known in quantum mechanics as the Feynman (or Dyson) path ordered exponential, in mathematics it is known as the Neumann or Peano series. Despite its age, the Neumann series seems to have only recently found use in the numerical analysis literature on ODEs, see [6,7,25,11,1], and references therein. It is easily seen that for $t \in [0, h]$ the Neumann series is dominated by the exponential series $\sum_{j=0}^{\infty}(rt)^j/j! = \mathrm{e}^{rt}$ with $r = \mathrm{Max}_{t\in[0,h]}\|A(t)\|$ (we assume A is continuous). Thus the Neumann series absolutely converges for all t, although if h is large many series terms may be needed, and upon truncation at the Nth term the tail is $\mathrm{O}(rt)^{N+1}$ (as $t \to 0$). Note that the Neumann series does not generally give a Lie group integrator, approximations of $y(t)$ obtained by truncation will generally not evolve in a matrix Lie group G even if $y(t)$ does.

The Magnus expansion, which respects Lie group structure, is another example of an integral series. It is briefly described below, and extensive discussions can be found in [12,14]. The fundamental solution of Eq. (4) on $[0, h]$ can be written in the form $\exp(\sigma)$, where $\sigma = \sigma_1 + \sigma_2 + \sigma_3 + \sigma_4 + \cdots$ is the Magnus series associated with Eq. (4). The first few terms are

$$\sigma_1 = \int_0^h A(t)\,\mathrm{d}t, \quad \sigma_2 = \frac{1}{2}\int_0^h \left[\int_0^t A(t_1)\,\mathrm{d}t_1, A(t)\right]\mathrm{d}t,$$

$$\sigma_3 = \frac{1}{4}\int_0^h \left[\int_0^t \left[\int_0^{t_1} A(t_2)\,\mathrm{d}t_2, A(t_1)\right]\mathrm{d}t_1, A(t)\right]\mathrm{d}t,$$

$$\sigma_4 = \frac{1}{12}\int_0^h \left[\int_0^t A(t_1)\,\mathrm{d}t_1, \left[\int_0^t A(t_1)\,\mathrm{d}t_1, A(t)\right]\right]\mathrm{d}t.$$

To avoid excessive detail we do not give further terms; however, it is useful to keep in mind that they are all obtained from $A(t)$ by repeated integrations and commutations. A linear change of variables extends these formulas to any interval $[t_n, t_{n+1}]$. Numerical Magnus integrators are based on truncation of the series and approximation of its head to obtain approximations of fundamental solutions on each grid subinterval. These are multiplied to form an approximation of the fundamental solution on a large interval. The local order of such integrators is given in the following theorem; if it is denoted by k then the global order is $k - 1$, see [9].

Theorem 1 (*adapted from Iserles and Nørsett [12]*). *Suppose* $A(t) = \mathrm{O}(t)$, *then*

$$\|\sigma(t) - \sigma_1(t)\| = \mathrm{O}(t^5), \tag{6}$$

$$\|\sigma(t) - (\sigma_1(t) + \sigma_2(t))\| = \mathrm{O}(t^7), \tag{7}$$

$$\|\sigma(t) - (\sigma_1(t) + \sigma_2(t) + \sigma_3(t) + \sigma_4(t))\| = \mathrm{O}(t^9). \tag{8}$$

If $\bar{\sigma}$ *is an approximation of the series head such that* $\|\sigma(t) - \bar{\sigma}(t)\| = \mathrm{O}(t^k)$ *then*

$$\|\exp(\sigma(t)) - \exp(\bar{\sigma}(t))\| = \mathrm{O}(t^k). \tag{9}$$

If $A(t) \in g$, *the Lie algebra corresponding to the Lie group* G, *then* $\exp(\bar{\sigma}(t)) \in G$ *together with the exact solution*.

Note that the order estimates in (6)–(8) may be viewed as pessimistic upper bounds; sometimes the truncated tail has even smaller norm as the discussion after Theorem 2 shows. The convergence of the Magnus and Neumann series is greatly enhanced if $\|A\|$ is small and if $A(t)$ has highly oscillatory entries. On the other hand, convergence is generally worse for smooth $A(t)$ with large norm. It is these features of the coefficient matrix which restrict the step size of Magnus and Neumann integrators applied directly to (1).

The basic integral which appears in the Magnus, or Neumann, series associated with the right correction equation is of the form

$$\int_0^h w(t)a(t)\,\mathrm{d}t, \tag{10}$$

with $w(t) = \exp(\mathrm{i}qt)$ (or $\cos(qt)$ or $\sin(qt)$), $a(t)$ a sufficiently smooth function, and large q causing severe integrand oscillation. To construct numerical integrators for the right correction equation we must address quadrature of such integrals. The oscillation will restrict "usual" quadrature, approximating the integral by a weighted sum of (*full*) integrand values, to small intervals. However, the methods described here do not suffer from the severe oscillation; on the contrary, it enhances their performance! In [10,13], Iserles and Nørsett treat this problem in great detail and give an extensive list of references.

An obvious suggestion is to approximate $a(t)$ with a polynomial $p(t)$ and evaluate $\int_0^h w(t)p(t)\,\mathrm{d}t$ analytically. One possibility, on which Filon quadrature is based [3], is that $p(t)$ will be an interpolation polynomial, i.e. it will equal $a(t)$ on a set of points in $[0, h]$. Careful choice of interpolation nodes yields surprisingly small error. We use the Filon–Legendre method; $p(t)$ is an mth degree interpolation polynomial with nodes on the $m + 1$ Legendre points, which are obtained by linearly mapping the roots of the $m + 1$ Legendre polynomial from $[-1, 1]$ to $[0, h]$. This defines a linear projector $Qa = p$. The quadrature error is $\mathrm{O}(h^{2m+3})$, therefore high accuracy is obtained with surprisingly low order polynomials requiring few evaluations of $a(t)$. The following explanation clarifies the mechanism at work here. On the interpolation nodes $a(t_j) - p(t_j) = 0$, but the nodes are the roots of $L_{m+1}(t)$, the Legendre polynomial of degree $m + 1$ on $[0, h]$. We can therefore write the quadrature error, $\int_0^h w(t)[a(t) - p(t)]\,\mathrm{d}t$, in the form $\int_0^h f(t)L_{m+1}(t)\,\mathrm{d}t$. But L_{m+1} is orthogonal to all polynomials of degree m or less. Hence all terms up to order m in the Taylor series of f contribute nothing to the error. Writing $L_{m+1}(t) = (t - t_1)\cdots(t - t_{m+1})$, where the roots are all in $[0, h]$, we see that the error is $\mathrm{O}(h^{2m+3})$. A different proof is given in [6], it is based on the following lemma.

Lemma 1 (*from Pruess [21]*). *Let* P *be the projector mapping a function* $f \in C^{2m+2}[-1, 1]$ *to the degree* m *polynomial* $p = Pf$ *such that* $p(x_j) = f(x_j)$ *on* $\{x_1, \ldots, x_{m+1}\}$ *the roots of the* $m + 1$ *degree Legendre polynomial. For this* P *there exists a constant* $K > 0$ *such that*

$$\left|\int_{-1}^{1} t^i(1 - P)(f)\,\mathrm{d}t\right| \leqslant K\|f^{(2m+2-i)}\|_\infty, \quad i = 0, \ldots, m. \tag{11}$$

The projector Q defined above satisfies a similiar system of inequalities obtained from (11) by a linear change of variable mapping $[-1, 1]$ to $[0, h]$. Our analysis of quadrature error given in [6] invokes only these inequalities and therefore it remains valid for approximation of $a(t)$ with different projectors, not necessarily of the interpolation type,

as long as they satisfy the same system of inequalities. In [21] a list of such projectors is given. Thus our analysis of quadrature error is valid not only for interpolation approximants $p(t)$ but for a wider class, including orthogonal projection of $a(t)$ onto spaces of polynomials which is so important in Section 5.

Integration by parts clearly shows how increasing q (severe oscillation) reduces the quadrature error

$$\int_0^h [a(t) - p(t)] \exp(\mathrm{i}qt)\, \mathrm{d}t = \sum_{n=0}^{N} (-1)^n \frac{1}{(\mathrm{i}q)^{n+1}} [(a(t) - p(t))^{(n)} \exp(\mathrm{i}qt)]_0^h + R_N. \tag{12}$$

R_N is a remainder term which is $o(q^{-N-1})$. In many cases this expansion extends to a convergent series, e.g. if exists a constant C such that $a^{(n)}(t) \leqslant C$ for all t, n. With our projector Q the first term in the expansion is non-zero, hence the error envelope decays like q^{-1}. In Filon–Lobatto quadrature, exposed in [10], the set of quadrature points includes the interval end points 0, h, thus the error envelope decays like q^{-2}. A generalization would be to choose polynomials satisfying the $2(n+1)$ conditions $p^{(k)}(0) = a^{(k)}(0)$, $p^{(k)}(h) = a^{(k)}(h)$, $k = 0, 1, \ldots, n$. These will give an error envelope decay of $q^{-(n+2)}$, see [8,3], and references therein.

Integral (10) arises from the first term in the Magnus (second in Neumann) series. The errors in approximation of higher terms is analysed in [6]; it is shown there that for fixed q the error is also $O(h^{2m+3})$. Fixing h, expansions similiar to (12), which are given in the sequel, show that the error is at worse bounded with increasing q.

3. RCMS applied to type A equations

A particular instance of Eq. (1) is the following:

Definition 1. Let G be a matrix Lie group with corresponding matrix Lie algebra g. Suppose that every element of g is diagonalizable with purely imaginary or zero eigenvalues. Equations of the form

$$y' = [\lambda A + A_1(t)]y, \tag{13}$$

with A, $A_1(t) \in g\ \forall t$, will be called type A equations.

G can be, for example, $SO(n)$ or $SU(n)$. There are two intrinsic scales in the problem. The first is $1/\lambda$, which determines the scale of oscillations in the solution, the second is the scale in which $A_1(t)$ changes. As λ increases the solution becomes highly oscillatory and the length of the first scale decreases while the second remains constant, see Fig. 1. An attempt to integrate Eq. (13) directly would be restricted to use small steps, standard schemes will suffer from the large values of solution derivatives (see Table 1), while Magnus and Neumann schemes will be affected by the large norm and non-oscillatory entries of the coefficient matrix in (13). RCMS achieves high accuracy with large steps for any λ. Guidelines for application are given in the following list.

1. Define a discretization of t. The step size is determined by $A_1(t)$ alone. This can be done a priori or adaptively during the run of the integrator.
2. In the nth grid interval define $\bar{A}_1$ as the value of $1/(t_{n+1} - t_n) \int_{t_n}^{t_{n+1}} A_1(t)\, \mathrm{d}t$ obtained by Gaussian quadrature of suitable order and $A_\lambda = A + (1/\lambda)\bar{A}_1$. Write Eq. (13) in the form
$$y' = [\lambda A_\lambda + (A_1(t) - \bar{A}_1)]y, \quad t \in [t_n, t_{n+1}].$$
3. Define the right correction u_n by $y(t_n, t) = \exp[(t - t_n)\lambda A_\lambda]u_n$, $t \in [t_n, t_{n+1}]$. u_n is a solution of
$$u_n' = B_n(t)u_n, \quad u_n(t_n) = E, \tag{14}$$
where
$$B_n(t) = \exp[-(t - t_n)\lambda A_\lambda](A_1(t) - \bar{A}_1) \exp[(t - t_n)\lambda A_\lambda].$$
4. Approximate the initial value problem (14) by replacing $(A_1(t) - \bar{A}_1)$ with the matrix $P(t)$ whose entries are degree m polynomial approximations of the entries of $(A_1(t) - \bar{A}_1)$ obtained as explained in Section 2. We shall shortly show that the choices $m = 1$ and $m = 2$ are suitable for fourth and sixth (global) order RCMS integrators.

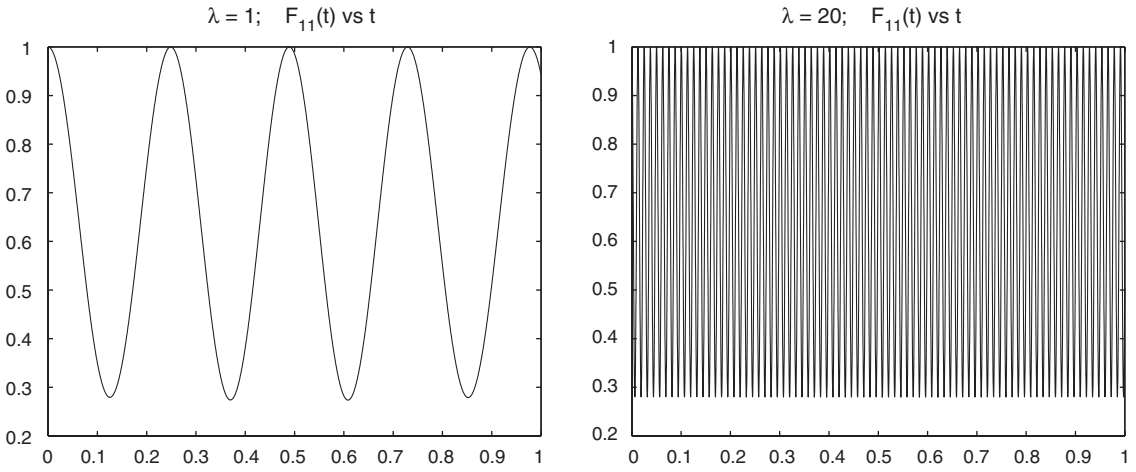

Fig. 1. Frenet–Serret, as λ grows the solution becomes increasingly oscillatory.

These graphs show the (1, 1) entry of the fundamental solution matrix, $y_{11}(0,t)$ vs $t \in [0,1]$. $\delta\tau(t) = \delta\kappa(t) = \sin(\pi t)^2$, $\kappa = 15\lambda$, $\tau = 20\lambda$, see Eq. (22). The graph on the left is for $\lambda = 1$ and on the right for $\lambda = 20$. The step size used in both cases was $h = \frac{1}{5000}$.

Table 1
RCMS performance versus standard methods

λ	*error*			N			*cpu time* (seconds)		
	RK4	RCMS4	ODE45	RK4	RCMS4	ODE45	RK4	RCMS4	ODE45
1	9.96×10^{-8}	8.7×10^{-8}	0.0028	985	21	161	4.51	0.26	0.94
10	9.86×10^{-8}	2.02×10^{-8}	0.028	17,007	43	1350	77.06	0.43	6.51
20	9.75×10^{-8}	8.9×10^{-8}	0.055	40,500	14	2665	177.6	0.14	12.8

Comparison of computational performance in approximation of the fundamental solution of Eq. (22) on [0, 1] with accuracy tolerance 10^{-7}, using fourth order RCMS (only the first Magnus series term), fourth order Runge Kutta and the Matlab solver ode45. For ode45 the absolute error tolerance was set using options = ('AbsTol', 1e-7). The parameters are $\delta\tau(t) = \delta\kappa(t) = \sin^2(\pi t)$, $\kappa = 15\lambda$, $\tau = 20\lambda$.

5. Obtain $\bar{u}_n$, an approximation of u_n, by calculating exactly the desired terms in the head of the Magnus series of the approximate i.v.p. using integration by parts.
6. The approximation of the fundamental solution of Eq. (13) on $[t_n, t_{n+1}]$ is $\bar{y}(t_n, t_{n+1}) = \exp[(t_{n+1} - t_n)\lambda A_\lambda]\bar{u}_n$. Obtain an approximation of $y(a,b)$, the fundamental solution of Eq. (13) on $[a,b]$, by time stepping $y(a,b) \approx \bar{y}(a,b) = \bar{y}(t_{N-1}, b)\bar{y}(t_{N-2}, t_{N-1}) \cdots \bar{y}(a, t_1)$.

The choice of step size in item 1 is not restricted by an increase of λ. On the contrary, errors are reduced by increasing oscillation and typically each step includes several solution "wavelengths". The form of Eq. (13) appearing in item 2 was chosen for the favourable effect of small $\|B_n\|$ (=O(h)) on Magnus series convergence. To obtain $P(t)$ our application uses the projector Q from Section 2 giving "Filon–Legendre" quadrature; other possibilities including non-interpolatory projectors are discussed there. The RCMS approximation $\bar{y}(a,b)$ is in G together with the exact solution $y(a,b)$.

Recall that all matrices are in g and therefore diagonalizable with purely imaginary eigenvalues. Diagonalizing, $T^{-1}AT = D$, $T_\lambda^{-1}A_\lambda T_\lambda = D_\lambda$, it is easily seen that as λ increases $A_\lambda \to A$, $T_\lambda \to T$, and therefore $\|T_\lambda\|$ is bounded for all relevant λ. We can write $B_n(t)$ in the form

$$B_n(t) = T_\lambda \exp[-(t - t_n)\lambda D_\lambda]T_\lambda^{-1}(A_1(t) - \bar{A}_1)T_\lambda \exp[(t - t_n)\lambda D_\lambda]T_\lambda^{-1}. \tag{15}$$

Let $\hat{B}_n(t) = T_\lambda^{-1} B_n(t) T_\lambda$; the entries of $\hat{B}_n(t)$ are

$$[\hat{B}_n(t)]_{ij} = \mathrm{e}^{\lambda(t-t_n)([D_\lambda]_i - [D_\lambda]_j)} [T_\lambda^{-1}(A_1(t) - \bar{A}_1) T_\lambda]_{ij}. \tag{16}$$

Eq. (16) shows clearly why the entries of $\hat{B}_n(t)$ and $B_n(t)$ are of the form $\mathrm{e}^{\mathrm{i}qt} a(t)$ (as in (10)) which is the basis for our approach to quadrature and error analysis. Note that the Magnus series $\hat{\sigma}$ and σ associated with $\hat{B}_n$ and B_n are related by the coordinate change $T_\lambda \hat{\sigma} T_\lambda^{-1} = \sigma$ and the same relation holds between individual series terms.

3.1. Error analysis

The local error of the integrator is

$$\begin{aligned} y(t_n, t_{n+1}) - \bar{y}(t_n, t_{n+1}) &= \exp[(t_{n+1} - t_n)\lambda A_\lambda] T_\lambda (\exp[\hat{\sigma}] - \exp[\bar{\sigma}]) T_\lambda^{-1} \\ &= T_\lambda \exp[(t_{n+1} - t_n)\lambda D_\lambda] (\exp[\hat{\sigma}] - \exp[\bar{\sigma}]) T_\lambda^{-1}, \end{aligned} \tag{17}$$

where $\bar{\sigma}$ is the approximation of $\hat{\sigma}$ obtained by truncation and polynomial approximation as described above. $\|T_\lambda\|$ and $\|\exp[(t_{n+1} - t_n)\lambda D_\lambda]\|$ are bounded independently of λ and of $h = t_{n+1} - t_n$, so the local error is determined by $\exp[\hat{\sigma}] - \exp[\bar{\sigma}]$. We examine two cases. Holding λ constant the error's order is studied as h is decreased. Fixing a discretization of t (which does not imply that the steps are uniform) the error's dependence on growing λ is examined.

3.1.1. Error dependence on step size (fixed λ)

By Theorem 1 $(\exp[\hat{\sigma}] - \exp[\bar{\sigma}])$ and $(\hat{\sigma} - \bar{\sigma})$ are of the same order in h. $(\hat{\sigma} - \bar{\sigma})$ is composed of the truncated tail of the series and of errors in approximation of the series head. Theorem 1 states that the truncated tail satisfies $\|\hat{\sigma} - \hat{\sigma}_1\| = \mathrm{O}(h^5)$ and $\|\hat{\sigma} - (\hat{\sigma}_1 + \hat{\sigma}_2)\| = \mathrm{O}(h^7)$. We turn to approximation of the series head. In Section 2 we have discussed why the error in approximation of the i, j entry of $\hat{\sigma}_1$ is

$$\left| \int_{t_n}^{t_{n+1}} \mathrm{e}^{\lambda(t-t_n)([D_\lambda]_i - [D_\lambda]_j)} [T_\lambda^{-1}(A_1(t) - \bar{A}_1 - P(t)) T_\lambda]_{ij} \, \mathrm{d}t \right| = \mathrm{O}(h^{2m+3})$$

and mentioned that errors in approximation of σ_2 (and higher terms) are also $\mathrm{O}(h^{2m+3})$. The order of error in approximation of the series head should be compatible with the order of the truncated Magnus series tail. Thus if only $\hat{\sigma}_1$ is included linear polynomials $(m = 1)$ should be used, if $\hat{\sigma}_1$ and $\hat{\sigma}_2$ are included then quadratic $(m = 2)$ polynomials should be used. The global error will be $\mathrm{O}(h^4)$ in the first case and $\mathrm{O}(h^6)$ in the second, or better. The discussion here is restricted to the first two Magnus terms, in [6] this is generalized.

3.1.2. Error dependence on λ (fixed steps)

Let $\bar{B}(t)$ be the matrix obtained from $\hat{B}(t)$ upon replacement of $A_1(t) - \bar{A}_1$ by $P(t)$. The terms of $\hat{\sigma}, \bar{\sigma}$ are constructed by repeated integration and commutation of $\hat{B}, \bar{B}$. Given (16), a brief reflection shows that if each integration is done by parts always taking integrals of exponents then it is possible to expand $\hat{\sigma}$ and $\bar{\sigma}$ in formal series of the form

$$\hat{\sigma} = \sum_{n=0}^{\infty} \frac{1}{\lambda^n} \hat{g}_n(\lambda, t), \quad \bar{\sigma} = \sum_{n=0}^{\infty} \frac{1}{\lambda^n} \bar{g}_n(\lambda, t), \tag{18}$$

where the entries of $\hat{g}_n(\lambda, t)$, $\bar{g}_n(\lambda, t)$ are bounded as $\lambda \to \infty$ (since the entries of T_λ, $\exp[\mathrm{i}\lambda(t - t_n) D_\lambda]$ are bounded as $\lambda \to \infty$). The definition of the matrix exponent gives the following useful relation:

$$\exp(\hat{\sigma}) - \exp(\bar{\sigma}) = \exp(\hat{g}_0) - \exp(\bar{g}_0) + \frac{1}{\lambda} \sum_{n=1}^{\infty} \frac{1}{n!} \sum_{k=1}^{n} \left(\hat{g}_0^{n-k} \hat{g}_1 \hat{g}_0^{k-1} - \bar{g}_0^{n-k} \bar{g}_1 \bar{g}_0^{k-1} \right) + \mathrm{O}\left(\frac{1}{\lambda^2} \right). \tag{19}$$

This expansion shows why RCMS local error does not increase with λ, the leading term is at worst bounded by a λ independent constant. Moreover, the discussion leading to Eq. (18) does not invoke Lie algebraic structure and could be applied to a Neumann series right correction scheme. Such a scheme applied to type A equations will have local error which is λ independent or decaying with increasing λ. Similiar analysis gives the same results for other types of equations.

To find the dependence of RCMS global error on λ we need to describe it in terms of local errors as in [9]. Let e_n, L_n denote the global and local errors, respectively, at the nth grid point. Assuming quadratic (and higher order) terms in e_{n-1} have negligible contribution to e_n we obtain

$$e_n = y(a,t_n)\sum_{k=0}^{n} y(a,t_{n-k})^{-1}L_{n-k} = \sum_{k=0}^{n} y(t_{n-k},t_n)L_{n-k}. \tag{20}$$

In addition to its dependence on local errors, the global error is influenced by the fundamental solutions $y(t_{n-k},t_n)$. In specific applications we will use the fact that $y(t_{n-k},t_n)$ is in G, and other information that will become available, to show that RCMS global error is also λ independent or decaying as λ grows.

3.2. Type A equations in so(3); Frenet–Serret equations

Consider $\gamma(t)$, a curve in $\mathbb{R}^3$ parameterized by arclength. At each t the tangent, normal, and binormal vectors are defined to be $\mathrm{T}=\gamma'$, $N=(1/\|\gamma''\|)\gamma''$, $\mathrm{B}=\mathrm{T}\times\mathrm{N}$. Viewing T, N, B as row vectors it is a classical result in differential geometry that they satisfy the following 3×3 matrix ODE, known as the Frenet–Serret equation (see [26])

$$\frac{\mathrm{d}}{\mathrm{d}t}\begin{pmatrix}\mathrm{T}\\ \mathrm{N}\\ \mathrm{B}\end{pmatrix} = \begin{pmatrix}0 & \kappa & 0\\ -\kappa & 0 & \tau\\ 0 & -\tau & 0\end{pmatrix}\begin{pmatrix}\mathrm{T}\\ \mathrm{N}\\ \mathrm{B}\end{pmatrix}. \tag{21}$$

The parameters $\kappa=\|\gamma''\|$ and $\tau=(1/\kappa^2)\det(\gamma'\gamma''\gamma''')$ are the curvature and torsion, respectively. The solution of (21) with initial condition $\mathrm{T}_0=\gamma'(0)$, $\mathrm{N}_0=(1/\|\gamma''(0)\|)\gamma''(0)$, $\mathrm{B}_0=\mathrm{T}_0\times\mathrm{N}_0$ evolves in $SO(3)$ and is called the osculating frame associated with γ. The family of curves in $\mathbb{R}^3$ related to γ by all possible rotations and translations is characterized by κ and τ. Thus knowing the fundamental solution of (21) is equivalent to knowing, up to integration of T, this family. For constant $\kappa,\tau>0$ the fundamental solution of (21) gives the family of all right handed helices (left handed if $\tau<0$) with pitch $\tan^{-1}(\tau/\kappa)$ and radius $\kappa/(\kappa^2+\tau^2)$. Frenet–Serret equations can describe different objects and processes, some applications in physics are given in [2,19] and the references therein.

We apply RCMS to the perturbed constant coefficient Frenet–Serret equation

$$y' = \begin{pmatrix}0 & \kappa+\delta\kappa(t) & 0\\ -\kappa-\delta\kappa(t) & 0 & \tau+\delta\tau(t)\\ 0 & -\tau-\delta\tau(t) & 0\end{pmatrix} y, \tag{22}$$

with τ, κ constant, $\tau^2+\kappa^2\gg 0$. The RCMS approximation resides in $SO(3)$ together with the exact solution. Thus, if (22) describes evolution of the osculating frame attached to a space curve, RCMS will preserve orthonormality. If (22) describes a two level quantum mechanical system in the Feynman Vernon Hellwarth representation [2], RCMS will conserve probability.

Define $\lambda=\sqrt{\kappa^2+\tau^2}$ and α such that $\cos(\alpha)=\kappa/\lambda$, $\sin(\alpha)=\tau/\lambda$. Let

$$A = \begin{pmatrix}0 & \cos\alpha & 0\\ -\cos\alpha & 0 & \sin\alpha\\ 0 & -\sin\alpha & 0\end{pmatrix},\quad A_1(t) = \begin{pmatrix}0 & \delta\kappa(t) & 0\\ -\delta\kappa(t) & 0 & \delta\tau(t)\\ 0 & -\delta\tau(t) & 0\end{pmatrix}.$$

Eq. (22) becomes

$$y' = [\lambda A + A_1(t)]y, \tag{23}$$

which is a type A equation since any non-zero matrix in $so(3)$ has one zero and two purely imaginary conjugate eigenvalues. As λ grows the solution of (23) exhibits increasing oscillation, see Fig. 1. Note that this need not occur in all entries of the fundamental solution, consider for example the slowly varying binormal and the rapidly oscillating tangent and normal of a tightly wound helix with small pitch.

To obtain an integrator with global error $\mathrm{O}(h^6)$, the steps in the general description of RCMS were followed with some minor variations.

1. Uniform grids with spacing h were used to simplify the programming; this choice can be refined.

2. $\bar{A}_1$ is defined by

$$\bar{A}_1 = \frac{1}{t_{n+1}-t_n}\,\text{Gaussian quadrature}\left(\int_{t_n}^{t_{n+1}} A_1(t)\,\mathrm{d}t\right) = \begin{pmatrix} 0 & \overline{\delta\kappa} & 0 \\ -\overline{\delta\kappa} & 0 & \overline{\delta\tau} \\ 0 & -\overline{\delta\tau} & 0 \end{pmatrix},$$

we have used three node Gaussian quadrature with $\mathrm{O}(h^7)$ error.

3. Write $\tilde{\kappa} = \kappa + \overline{\delta\kappa}$, $\tilde{\tau} = \tau + \overline{\delta\tau}$, $\tilde{\lambda} = \sqrt{\tilde{\kappa}^2 + \tilde{\tau}^2}$ and define $\tilde{\alpha}$ by $\cos\tilde{\alpha} = \tilde{\kappa}/\tilde{\lambda}$, $\sin\tilde{\alpha} = \tilde{\tau}/\tilde{\lambda}$. Let

$$R = \begin{pmatrix} 0 & \cos\tilde{\alpha} & \sin\tilde{\alpha} \\ 1 & 0 & 0 \\ 0 & -\sin\tilde{\alpha} & \cos\tilde{\alpha} \end{pmatrix}, \quad \text{then} \quad R^{-1}[\lambda A + \overline{A}_1]R = \tilde{A} = \begin{pmatrix} 0 & -\tilde{\lambda} & 0 \\ \tilde{\lambda} & 0 & 0 \\ 0 & 0 & 0 \end{pmatrix}. \tag{24}$$

Defining $z_n = R^{-1}u_n R$, after some calculation we obtain

$$z_n' = \begin{pmatrix} 0 & -f_1(t) & \cos(\tilde{\lambda}t)f_2(t) \\ f_1(t) & 0 & -\sin(\tilde{\lambda}t)f_2(t) \\ -\cos(\tilde{\lambda}t)f_2(t) & \sin(\tilde{\lambda}t)f_2(t) & 0 \end{pmatrix} z_n, \quad t \in [t_n, t_{n+1}], \tag{25}$$

where $f_1(t) = \cos\tilde{\alpha}\,(\delta\kappa(t) - \overline{\delta\kappa}) + \sin\tilde{\alpha}\,(\delta\tau(t) - \overline{\delta\tau})$, $f_2(t) = \cos\tilde{\alpha}\,(\delta\tau(t) - \overline{\delta\tau}) - \sin\tilde{\alpha}\,(\delta\kappa(t) - \overline{\delta\kappa})$.

4. $f_1(t)$ and $f_2(t)$ are approximated by the quadratic interpolation polynomials $p_1 = Qf_1$ and $p_2 = Qf_2$. Relevant subroutines return the coefficients of p_1, p_2 using three function evaluations of f_1 and f_2.
5. Replacing f_1, f_2, by p_1, p_2, in Eq. (25) the first two terms in the Magnus series are explicitly calculated to obtain $\bar{\sigma}$. The formulas giving $\bar{\sigma}$ as a function of h, $\tilde{\lambda}$ and of the coefficients in p_1, p_2 appear in Appendix A.
6. The approximation of u_n is $R\exp(\bar{\sigma})R^{-1}$ and the RCMS approximation of the solution of Eq. (22) on the nth grid interval is

$$\bar{y}(t_n, t_{n+1}) = R\exp(h\tilde{A})\,\exp(\bar{\sigma})R^{-1}, \tag{26}$$

the local error is $\mathrm{O}(h^7)$. The approximations from successive grid intervals are composed to obtain $\bar{y}(a,b)$, a sixth order approximation of $y(a,b)$, the fundamental solution of (22) on an interval $[a,b]$.

Aparicio et al. [1] study equations very similiar to (13). They also use precalculated formulas for approximation of the Magnus and Neumann series. However, these are applied directly to (13) rather than to right corrections. Consequently the errors of the integrators in [1] grow with λ.

To address the error's independence on λ we proceed as outlined in Section 3.1.2. The first step is expanding σ and $\bar{\sigma}$ in power series of $1/\tilde{\lambda}$. Integrating by parts, we obtain the head of the $1/\tilde{\lambda}$ expansion of σ_1, the first term in the Magnus series associated with Eq. (25). The same analysis applies to $\bar{\sigma}_1$ with p_1 and p_2 replacing f_1 and f_2.

$$\sigma_1 = \begin{pmatrix} 0 & -\int_0^h f_1(t)\,\mathrm{d}t & 0 \\ \int_0^h f_1(t)\,\mathrm{d}t & 0 & 0 \\ 0 & 0 & 0 \end{pmatrix} + \frac{1}{\tilde{\lambda}}\begin{pmatrix} 0 & 0 & s_1(h) \\ 0 & 0 & s_2(h) \\ -s_1(h) & -s_2(h) & 0 \end{pmatrix} + \text{h.o.t.}, \tag{27}$$

where $s_1(h) = f_2(h)\sin(\tilde{\lambda}h)$ and $s_2(h) = -(f_2(0) - \cos(\tilde{\lambda}h)f_2(h))$. It can be shown that all higher Magnus series terms do not contribute to the zeroth term in the $1/\tilde{\lambda}$ expansion of σ and $\bar{\sigma}$. Moreover, an infinite number of series terms contribute to the $\mathrm{O}(1/\tilde{\lambda})$ term and hence we do not attempt to calculate it (the analysis in [20] may be possibly used to refine this). As in Eq. (18) we can write

$$\sigma = g_0 + \mathrm{O}\left(\frac{1}{\tilde{\lambda}}\right), \quad \bar{\sigma} = \bar{g}_0 + \mathrm{O}\left(\frac{1}{\tilde{\lambda}}\right) \quad \text{where } g_0 = \begin{pmatrix} 0 & -\int_0^h f_1(t)\,\mathrm{d}t & 0 \\ \int_0^h f_1(t)\,\mathrm{d}t & 0 & 0 \\ 0 & 0 & 0 \end{pmatrix}.$$

But $\int_0^h p_1(t)\,\mathrm{d}t = 0$ since $\overline{\delta\kappa}$ and $\overline{\delta\tau}$ are obtained by three node Gaussian quadrature and the same interpolation nodes are used for p_1. Hence $\bar{g}_0 = 0$ and by Eq. (19), (26) the local error is

$$R\exp(h\tilde{A})(\exp(\sigma) - \exp(\bar{\sigma}))R^{-1} = R\exp(h\tilde{A})(\exp(g_0) - I)R^{-1} + \mathrm{O}\left(\frac{1}{\tilde{\lambda}}\right), \tag{28}$$

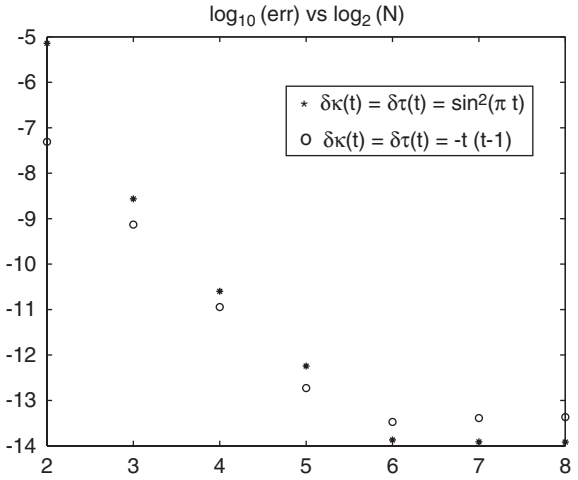

Fig. 2. Frenet–Serret, observed h dependence of RCMS error agrees with analysis.

The graph marked by circles shows $\log_{10}$ of the error versus $\log_2$ of the number of grid intervals, $\log_{10}(\|y(0,1)-\bar{y}(0,1)\|)$ vs $\log_2(N)$, in RCMS applied to Eq. (22) with $\kappa=10$, $\tau=6$, $\delta\kappa(t)=\delta\tau(t)=-t(t-1)$. For the above choice of $\delta\kappa(t)$, $\delta\tau(t)$ the terms in the Magnus series head are evaluated exactly, so only the truncated tail contributes to the error. The graph marked in stars is for $\kappa=10$, $\tau=6$, $\delta\kappa(t)=\delta\tau(t)=\sin^2(\pi t)$. For this choice of $\delta\kappa(t)$, $\delta\tau(t)$, the RCMS error includes contributions from errors in approximating the Magnus series head. As our analysis predicts the global error is $O(h^6)$ in both cases.

The global error is given in Eq. (20). Since the $y(t_{n-k}, t_n)$ are rotations and the leading terms in the local errors are λ independent, so is the leading part of the global error.

3.2.1. Results

We compare the performance of fourth order RCMS, taking just the first Magnus series term, with the Matlab solver ode45 and with the standard fourth order Runge Kutta method from [24] both applied directly to Eq. (22). Results are summarized in Table 1. The *error* is $\|y(0,1)-\bar{y}(0,1)\|$ where $y(0,1)$ is a high accuracy approximation of the exact fundamental solution at $t=1$. $\bar{y}(0,1)$ is the approximation of the fundamental solution at $t=1$ obtained with RCMS, Runge Kutta or ode45. N is the number of steps taken by the different integrators. The values of N appearing in the table for RCMS4 and for RK4 were obtained by a binary search to find the smallest N for which $error<10^{-7}$. ode45 was run with the absolute error tolerance set to 10^{-7}. The *cpu time* was evaluated for a Matlab 6 implementation using the Matlab cpu time command. This comparison is a striking illustration of RCMS performance; note that for $\lambda=20$ the (1, 1) entry of the fundamental solution has approximately five "wavelengths" in each RCMS step. A serious comparison to ODE45, and other ODE software, must address issues of automatic step size control. We avoid this, but note in passing that the results in Table 1 and the extensive discussion of error accumulation in classical schemes (with fixed steps, and with step size control) given in [9] do indicate the need for accessible software for oscillatory ODEs.

In Fig. 2 numerical results are given for $\kappa=10$, $\tau=6$, $t\in[0,1]$, $\delta\kappa(t)=\delta\tau(t)=-t(t-1)$ and $\delta\kappa(t)=\delta\tau(t)=\sin^2(\pi t)$. The graphs show $\log_{10}(\|y(0,1)-\bar{y}(0,1)\|_2)$ versus $\log_2(N)$, where $\bar{y}(0,1)$ was obtained with grids having $N=2^m+1$ points, $m=2,\ldots,8$. As predicted by our analysis the global error is $O(h^6)$ in both cases.

In Fig. 3 the λ independence of local error and global error is illustrated for $\delta\tau(t)=\delta\kappa(t)=2\exp(10t)\sin^2(\pi t)$, $\kappa=15\lambda$, $\tau=20\lambda$ and $\lambda\in[1,5\times10^4]$. The graphs show that as λ grows the norm of the global and local error approaches a λ independent constant.

4. RCMS applied to the 1D Schrödinger equation

The 1D Schrödinger eigenproblem is fundamental in quantum mechanics and other areas. References to some applications, together with those for other Sturm Liouville problems, can be found in [20,23]. We consider the "regular" version of the problem [23] which can be stated in vector form thus:

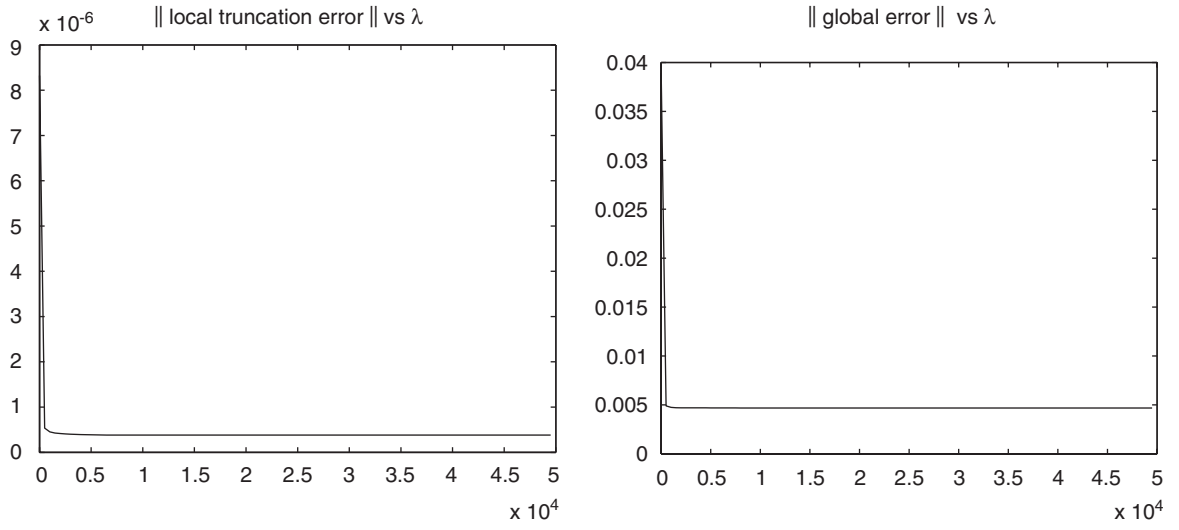

Fig. 3. Frenet–Serret, λ independence of RCMS error.

The local and global errors in approximation of the fundamental solution were obtained for RCMS applied to Eq. (22). The results are for $\delta\tau(t) = \delta\kappa(t) = 2\exp(10t)\sin(\pi t)^2$, $\kappa = 15\lambda$, $\tau = 20\lambda$, $\lambda \in [1, 5 \times 10^4]$. The local error was obtained by RCMS approximating $y(0, 0.1)$ using just one step, $h = 0.1$, and comparing to a high accuracy approximation of $y(0, 0.1)$ (obtained with 10 RCMS steps $h = 0.01$). The global error was obtained by RCMS approximating $y(0, 1)$ using 10 steps, $h = 0.1$, and comparing to a high accuracy approximation of $y(0, 1)$ (obtained with 500 RCMS steps $h = \frac{1}{500}$). On the left ‖local error‖ vs λ is shown and on the right ‖global error‖ vs λ. In both cases the errors are λ independent as the analysis in Section 3.2.1 predicts.

Given a finite closed interval $[a, b]$ *and a continuous function* $V(x)$ *on it, find all eigenvalues* λ *for which there exists a nontrivial solution to the b.v.p.*

$$y' = \begin{pmatrix} 0 & 1 \\ V(x) - \lambda & 0 \end{pmatrix} y, \quad x \in (a, b), \tag{29}$$

$$B_a y(a) + B_b y(b) = 0, \quad B_a, B_b \in \mathbb{R}^{2\times 2}. \tag{30}$$

For each eigenvalue find the corresponding eigenfunction.

In quantum mechanics textbooks (29) usually appears in the form $-\psi''(x) + V(x)\psi(x) = \lambda\psi(x)$ which is the 1D version of $\hat{H}\psi = \lambda\psi$ with $\hat{H} = -\Delta + V$.

Let $y(\lambda, a, b)$ be the fundamental solution of (29) on $[a, b]$. Then (30) gives $[B_a + B_b y(\lambda, a, b)]y(a) = 0$. So the problem of finding eigenvalues is equivalent to finding all λ such that

$$\det[B_a + B_b y(\lambda, a, b)] = 0. \tag{31}$$

An essential step used by all "shooting" algorithms, searching for solutions of (31), is the integration of (29) or an equivalent equation to obtain $y(\lambda, a, b)$. Note that the coefficient matrix in (29) is in $sl(2)$ (trace $= 0$) hence the fundamental solution is in $SL(2)$ (det $=1$).

Several kinds of difficulty arise. In the case $V(x) - \lambda \gg 0$ integrators applied to (29) are susceptible to numerical instability. The discussion in [7,6], and the results in [15], strongly indicate that RCMS and other right correction integral series schemes can perform well in this regime.

Here we concentrate on $V(x) - \lambda \ll 0$, where the solution is severely oscillatory. As λ grows the solution "wavelength" approaches $2\pi/\sqrt{\lambda}$ and in the search for large eigenvalues a naive integrator will be forced to make increasingly smaller steps. To avoid this some algorithms use the scaled Prüfer transformation, see [23] for a thorough discussion. In certain problems, where a good scaling function is heuristically found, this removes the oscillations and allows large x steps to be taken. However, the scope of this approach is limited by the fact that there is no general method for finding the scaling function.

In [21] Pruess suggests to solve the eigenvalue problem by *approximating the differential equation* (29). This is done by replacing $V(x)$ with piecewise polynomial approximations. For conventional numerical integrators solving the approximate problem, with polynomials of order greater than zero, is no easier than the original. Thus until recently only piecewise constant polynomials were used in practical software packages (SLEDGE [22]), because for these (29) is easily analytically integrated. For such piecewise constant methods (PWCM) the step size is not restricted by the oscillations in $y(x)$ as long as the matrices B_a, B_b have zero bottom rows, i.e. the boundary conditions include only the first component of vector solutions of Eq. (29). The main disadvantage of PWCM is their low order, with global error $O(h^2)$. To overcome this repeated Richardson extrapolation is used in [22].

Recently two approaches, of Moan [20] and Ixaru et al. [15], have been suggested towards the realization of the idea of approximating Eq. (29) with *high order* piecewise polynomial $V(x)$. Moan [20] applies Magnus series integrators *directly* to Eq. (29) with piecewise polynomial $V(x)$. The discussion in Section 2 implies that this is not recommended because the norm of the matrix in (29) grows large with increasing λ while its entries remain non-oscillatory. Indeed, despite a clever method for analytic evaluation of subseries of the Magnus series, the increase of the integrators' error with λ is not eliminated.

Ixaru et al. [15] apply an algorithm that is closely related to our work, so we discuss it in some detail. The fundamental solution for Eq. (29) on the nth grid interval is regarded in [15] as the limit of the series

$$y(\lambda, x_n, x) = P_0(x) + P_1(x) + P_2(x) + \cdots, \quad x \in [x_n, x_{n+1}], \tag{32}$$

where

$$P_0(x) = \exp\left[(x - x_n)\begin{pmatrix} 0 & 1 \\ V_n - \lambda & 0 \end{pmatrix}\right],$$

$$P_k' = \begin{pmatrix} 0 & 1 \\ V_n - \lambda & 0 \end{pmatrix} P_k + \begin{pmatrix} 0 & 0 \\ V(x) - V_n & 0 \end{pmatrix} P_{k-1}, \quad P_k(x_n) = 0, \tag{33}$$

i.e. (32) is a perturbation series solution for (29) regarding $V(x) - V_n$ as a perturbation of V_n, a constant approximation of $V(x)$ on $[x_n, x_{n+1}]$. The description of series (32) given in [15] is

$$P_k(x) = P_0(x) \int_{x_n}^{x} P_0^{-1}(s) \begin{pmatrix} 0 & 0 \\ V(s) - V_n & 0 \end{pmatrix} P_{k-1}(s)\, \mathrm{d}s \tag{34}$$

and integrators based on it are called piecewise perturbation methods (PPM). To obtain a different viewpoint note that

$$P_1(x) = P_0(x) \int_{x_n}^{x} B_n(s_1)\, \mathrm{d}s_1 \tag{35}$$

and for $k = 2, 3, \ldots$

$$P_k(x) = P_0(x) \int_{x_n}^{x} B_n(s_1) \int_{x_n}^{s_1} B_n(s_2) \ldots \int_{x_n}^{s_{k-1}} B_n(s_k)\, \mathrm{d}s_k \ldots \mathrm{d}s_2\, \mathrm{d}s_1, \tag{36}$$

where B_n is precisely the right correction equation matrix of coefficients from Eq. (39). Thus, the piecewise perturbation approach in [15] may be viewed as a Neumann series applied to the right correction equation (39).

This observation places RCMS and the PPM integrator together in the family of *right correction integral series* integrators. In such integrators $V(x)$ is replaced by a polynomial approximation and the resulting series terms are evaluated analytically. The advantages of this approach stand out. Taking a large number of terms can give a very high order of accuracy. Moreover, if $V_n - \lambda \ll 0$ the oscillations in the entries of $B_n(x)$ reduce all contributions to the error, those arising from truncation of the series and those arising from approximations of terms in its head. The major difference is that the PPM integrator does not respect evolution in $SL(2)$. The excellent performance of the eigenvalue search algorithm in [15] is a convincing illustration of the high efficiency of right correction integral series schemes. We note in passing that our analysis indicates the possibility that lower order polynomials may have been used in [15] with the same order of error. In [16] Ixaru et al. expand their method to general regular Sturm Liouville problems using the Liouville transformation.

We construct an RCMS integrator for x marching in the 1D Schrödinger equation. The implementation is only for λ such that $V(x) - \lambda < 0\ \forall x$ but it is possible to extend for general λ. The integrator preserves $SL(2)$ structure,

has high order with respect to the step size and its error does not depend on positive powers of λ. This means that the step size is determined only with respect to the scale on which $V(x)$ changes with no need to decrease it as $|\lambda|$ grows.

Let us introduce a piecewise constant approximation of $V(x)$ whose value on $[x_n, x_{n+1}]$ is denoted by V_n, in our application $V_n = 1/(x_{n+1} - x_n)$ Gauss quadrature ($\int_{x_n}^{x_{n+1}} V(\xi)\,\mathrm{d}\xi$). On this interval Eq. (30) can be written as

$$y' = \left[\begin{pmatrix} 0 & 1 \\ V_n - \lambda & 0 \end{pmatrix} + \begin{pmatrix} 0 & 0 \\ V(x) - V_n & 0 \end{pmatrix}\right] y, \quad x \in [x_n, x_{n+1}]. \tag{37}$$

The right correction u_n is defined by

$$y(\lambda, x_n, x) = \exp\left[(x - x_n)\begin{pmatrix} 0 & 1 \\ V_n - \lambda & 0 \end{pmatrix}\right] u_n(x), \quad x \in [x_n, x_{n+1}]. \tag{38}$$

Then

$$u_n' = B_n(x) u_n, \quad x \in [x_n, x_{n+1}], \tag{39}$$

with

$$B_n(x) = \exp\left[-(x - x_n)\begin{pmatrix} 0 & 1 \\ V_n - \lambda & 0 \end{pmatrix}\right]\begin{pmatrix} 0 & 0 \\ V(x) - V_n & 0 \end{pmatrix}\exp\left[(x - x_n)\begin{pmatrix} 0 & 1 \\ V_n - \lambda & 0 \end{pmatrix}\right]. \tag{40}$$

Denoting $q_n = \sqrt{\lambda - V_n}$, after some calculations it is found that for $\lambda - V_n > 0$

$$B_n(x) = (V(x) - V_n)\begin{pmatrix} -\dfrac{1}{2q_n}\sin[2(x - x_n)q_n] & -\dfrac{1}{q_n^2}\sin^2[(x - x_n)q_n] \\ \cos^2[(x - x_n)q_n] & \dfrac{1}{2q_n}\sin[2(x - x_n)q_n] \end{pmatrix}. \tag{41}$$

The RCMS integrator implemented in this work for the 1D Schrödinger equation consists of the following steps:

1. As in our treatment of Frenet–Serret equations, uniform grids are chosen to simplify the programming. This is not necessary and could be refined.
2. V_n, an approximation of $(1/(x_{n+1} - x_n)) \int_{x_n}^{x_{n+1}} V(\xi)\,\mathrm{d}\xi$, is calculated using four node Gaussian quadrature.
3. The four coefficients in the cubic polynomial approximation of $V(x) - V_n$, obtained using the projector Q from Section 2, are calculated. For this the four function evaluations from item 2 are used.
4. These four coefficients are input, together with q_n, h, to precalculated formulas, given in Appendix A, that return $\bar{\sigma}$, the approximation of the Magnus series truncated after the first two terms.
5. Finally, the ninth order approximation of $y(\lambda, x_n, x_{n+1})$ is

$$\bar{y}(\lambda, x_n, x_{n+1}) = \exp\left[(x_{n+1} - x_n)\begin{pmatrix} 0 & 1 \\ V_n - \lambda & 0 \end{pmatrix}\right]\exp(\bar{\sigma}).$$

6. To generate an eighth order approximation of the fundamental solution of Eq. (29) on the whole interval $[a, b]$, the $\bar{y}(\lambda, x_n, x_{n+1})$ from each subinterval are multiplied.

It should be noted that the very fact that makes the formulas in item 4 useful for large q_n, the appearance of q_n in the denominators, causes numerical instability for λ close to V_n, i.e. $0 < q_n \ll 1$. In this case the entries of B_n are slowly varying and simple Gaussian quadrature can be used to evaluate the integrals in a Magnus integrator applied directly to Eq. (29). Note also that although only the first two terms in the Magnus series, σ_1, σ_2, are included, the integrator is eighth order, while Theorem 1 guarantees only sixth order. This is explained next.

4.1. Error dependence on step size (fixed λ)

The following surprising theorem is proven in [6].

Theorem 2. *Let σ_3 and σ_4 be the third and fourth terms in the Magnus series. For the right correction equation* (39) *corresponding to the* 1D *Schrödinger equation, the joint contribution of these two terms to the Magnus series is* $O(h^9)$ *i.e.*

$$\|\sigma_3 + \sigma_4\| = O(h^9).$$

Note that in the Frenet–Serret equation this phenomenon did not occur, truncation of the right correction Magnus series after the first two terms gave a sixth order integrator. Theorem 2 together with the results quoted in Theorem 1 implies that if the Magnus series is truncated after the first two terms the tail is $O(h^9)$. Our choice of polynomial approximation of $V(x) - V_n$ ensures that σ_1 and σ_2 are approximated with an $O(h^9)$ error. The resulting (global) order of the integrator is 8.

4.2. Error dependence on λ (fixed steps)

Although the 1D Schrödinger equation is not a type A equation, the discussion in Section 3 applies since the form of entries of the matrix B_n is the same as in Eq. (16). So it is possible to expand σ and $\bar{\sigma}$ in the form $\sigma = \sum_{j=0}^{\infty} q_n^{-j} g_j(q_n, t)$ and $\bar{\sigma} = \sum_{j=0}^{\infty} q_n^{-j} \bar{g}_j(q_n, t)$.

To obtain the $1/q_n$ dependence of the local error we calculate $g_0, g_1, g_2, \bar{g}_0, \bar{g}_1, \bar{g}_2$. Using integration by parts the contribution of σ_1, σ_2 to g_0, g_1, g_2 is explicitly found. Integration by parts also shows that the leading terms in σ_3, σ_4 are $O(1/q_n^3)$. In [6] it is proved that all higher Magnus series terms also contributed nothing to g_0, g_1, g_2. Thus

$$g_0 = \begin{pmatrix} 0 & 0 \\ A & 0 \end{pmatrix}, \quad g_1 = \begin{pmatrix} 0 & 0 \\ B & 0 \end{pmatrix}, \quad g_2 = \begin{pmatrix} C - D & -A \\ E - AC - AD & D - C \end{pmatrix}, \tag{42}$$

where

$$A = \frac{1}{2} \int_{x_n}^{x_{n+1}} [V(x) - V_n]\,dx, \quad C = \frac{1}{4} \cos(2h_n q_n)[V(x_{n+1}) - V_n],$$
$$B = \frac{1}{4} \sin(2h_n q_n)[V(x_{n+1}) - V_n], \quad D = \frac{1}{4} [V(x_n) - V_n],$$
$$E = \frac{1}{8} \left[\int_{x_n}^{x_{n+1}} (V(x) - V_n)^2\,dx + \cos(2h_n q_n) V'(x_{n+1}) - V'(x_n) \right].$$

$\bar{g}_0, \bar{g}_1, \bar{g}_2$ are obtained similarly with the cubic polynomial $p(x)$ replacing $V(x) - V_n$. We define $e(x) = V(x) - V_n - p(x)$ and note that

$$\exp\left[x \begin{pmatrix} 0 & 1 \\ V_n - \lambda & 0 \end{pmatrix} \right] = \begin{pmatrix} \cos(xq_n) & 1/q_n \sin(xq_n) \\ -q_n \sin(xq_n) & \cos(xq_n) \end{pmatrix}, \quad V_n - \lambda > 0. \tag{43}$$

Explicitly writing the $O(1/\lambda^2)$ terms in Eq. (19) we obtain

$$\text{local error} = \begin{pmatrix} 0 & 0 \\ M_n & 0 \end{pmatrix} + \frac{1}{q_n} \begin{pmatrix} N_n & 0 \\ P_n & N_n \end{pmatrix} + \frac{1}{q_n^2} \begin{pmatrix} Q_n & -M_n \\ R_n & K_n \end{pmatrix} + O\left(\frac{1}{q_n^3} \right), \tag{44}$$

where

$$M_n = \frac{1}{2} \cos(h_n q_n) \int_{x_n}^{x_{n+1}} e(x)\,dx, \quad N_n = \frac{1}{2} \sin(h_n q_n) \int_{x_n}^{x_{n+1}} e(x)\,dx,$$
$$P_n = \tfrac{1}{4} \sin(h_n q_n)[e(x_{n+1}) - e(x_n)], \quad K_n = \tfrac{1}{4} \cos(h_n q_n)(e(x_n) - \cos(2h_n q_n) e(x_{n+1})),$$
$$Q_n = \tfrac{1}{4} \cos(h_n q_n)[e(x_{n+1}) - e(x_n)]. \tag{45}$$

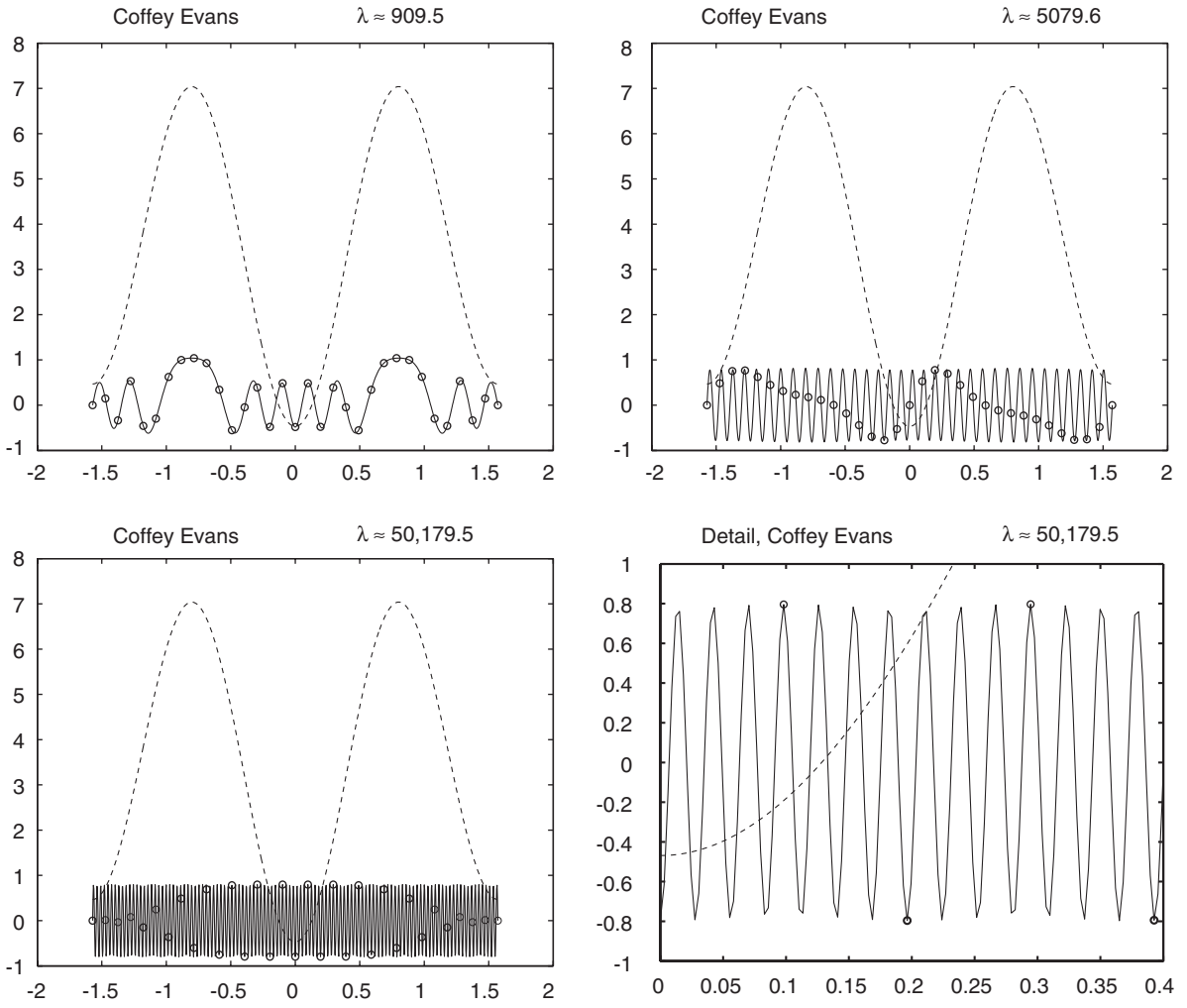

Fig. 4. One-dimensional Schrödinger, as λ increases solutions become increasingly oscillatory and RCMS behaviour improves.

Shown here are high accuracy approximations of eigenfunctions (continuous lines) and RCMS approximations of them (∘) for the Coffey–Evans potential $V(x)=-2\beta\cos(2x)+\beta^2\sin^2(2x), x\in[-\pi/2,\pi/2], \beta=30$, in the 1D Schrödinger equation with boundary conditions $y(-\pi/2)=y(\pi/2)=0$. Also shown is $\frac{1}{128}V(x)$ (broken line). The $\frac{1}{128}$ factor is just to normalize $V(x)$ to the scale of the figure. The graphs were constructed with the following choices of λ which are all approximate eigenvalues: top left: $\lambda=909.4810465034$; top right: $\lambda=5079.573751132997$. Bottom left and right: $\lambda=50,179.518034624$. The bottom right figure is a detail of the bottom left. Notice how the number of eigenfunction "wave lengths" per RCMS step increases with λ. In contrast to conventional integrators RCMS performance improves with increasing λ instead of deteriorating, with no increase of work. The maximal error of the RCMS approximation is bounded by 6×10^{-4}, 1.11×10^{-6}, 7.5×10^{-8}, respectively (for increasing values of λ), and step length is $\pi/32$ in all cases. The high accuracy eigenfunctions where constructed using RCMS with step size $\pi/1024$.

R_n can be calculated explicitly but it is cumbersome and unnecessary because the corresponding lower order entries dominate.

To find the dependence of global error on λ recall Eq. (20) describing the dependence of global error on local errors. Let $\tilde{V}_n=(1/(x_{n+1}-x_n))\int_{x_n}^{x^{n+1}}V(x)\,\mathrm{d}x$ exactly, $\tilde{q}_n=\sqrt{\lambda-\tilde{V}_n}$, $h_j=x_{j+1}-x_j$. Taking $V_n=\tilde{V}_n$, we see that A from (42) is zero hence $\lim_{\lambda\to\infty}u_n=E$, and so

$$\lim_{\lambda\to\infty}y(\lambda,x_j,x_{j+1})=\begin{pmatrix}\cos(h_j\tilde{q}_j) & \dfrac{1}{\tilde{q}_j}\sin(h_j\tilde{q}_j)\\ -\tilde{q}_j\sin(h_j\tilde{q}_j) & \cos(h_j\tilde{q}_j)\end{pmatrix}. \tag{46}$$

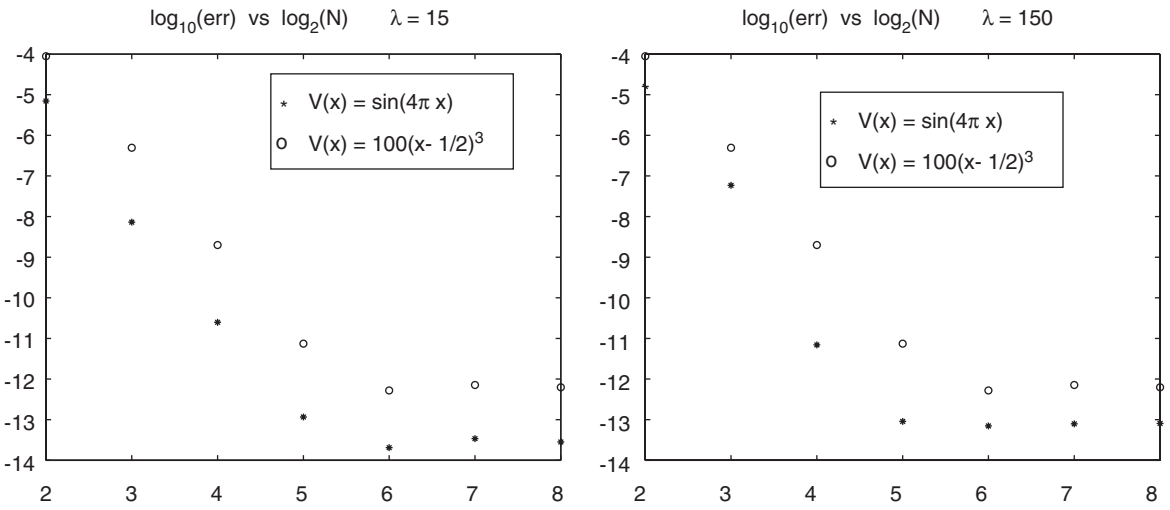

Fig. 5. One-dimensional Schrödinger, dependence of RCMS error on step size h.

The graphs show $\log_{10}(\|y(\lambda, 0, 1) - \bar{y}(\lambda, 0, 1)\|)$ vs $\log_2(N)$ (N is the number of grid intervals), with $\lambda = 15, 150$, in RCMS applied to the 1D Schrödinger equation with $V(x) = \sin(4\pi x)$ $(*)$, and $V(x) = 100(x - 1/2)^3$ $(\circ)$, $x \in [0, 1]$. The graphs illustrate that for fixed λ the global error is $O(h^8)$ as predicted in Section 4.

Thus, keeping terms up to $1/q_n$, as $\lambda \to \infty$ Eq. (20) becomes

$$e_n \approx \sum_{k=0}^{n} \prod_{j=n-k}^{n-1} \begin{pmatrix} \cos(h_j\tilde{q}_j) & \frac{1}{\tilde{q}_j}\sin(h_j\tilde{q}_j) \\ -\tilde{q}_j \sin(h_j\tilde{q}_j) & \cos(h_j\tilde{q}_j) \end{pmatrix} \left[\begin{pmatrix} 0 & 0 \\ M_{n-k} & 0 \end{pmatrix} + \frac{1}{q_{n-k}} \begin{pmatrix} N_{n-k} & 0 \\ P_{n-k} & N_{n-k} \end{pmatrix} \right]. \tag{47}$$

Following the matrix multiplications it is easily seen that as $\lambda \to \infty$ the global error is

$$e_n = \begin{pmatrix} O\left(\frac{1}{\sqrt{\lambda}}\right) & O\left(\frac{1}{\lambda}\right) \\ O(1) & O\left(\frac{1}{\sqrt{\lambda}}\right) \end{pmatrix}. \tag{48}$$

This was confirmed numerically.

4.3. Results

Fig. 4 shows eigenfunctions and their RCMS approximations, corresponding to eigenvalues $\lambda \approx 909.4810$, $\lambda \approx 5079.5737$, $\lambda \approx 50, 179.5180$ for the Coffey–Evans problem (see [23]) $V(x) = -2\beta\cos(2x) + \beta^2\sin^2(2x)$, $x \in [-\pi/2, \pi/2]$, $\beta = 30$, with boundary conditions $y(-\pi/2) = y(\pi/2) = 0$. The figures illustrate the increasing oscillations in the solutions of the 1D Schrödinger equation and the increasing accuracy of RCMS as λ increases. In Fig. 5 results are given for $V(x) = 100(x - \frac{1}{2})^3$ and $V(x) = \sin(4\pi x)$ on [0,1]. The graphs in Fig. 5 show $\log_{10}(\|y(\lambda, 0, 1) - \bar{y}(\lambda, 0, 1)\|)$ versus $\log_2(N)$, N being the number of grid intervals. $y(\lambda, 0, 1)$ is a high accuracy approximation of the exact value of the fundamental solution at $x = 1$ obtained with a very fine grid, $h = 2^{-9}$. $\bar{y}(\lambda, 0, 1)$ is the RCMS approximation of the fundamental solution at $x = 1$ obtained with coarser grids $N = 2^m + 1$, $m = 2, \ldots, 8$. As expected, the global error is $O(h^8)$ agreeing with our predictions.

Because of our choice of $p(x)$, all terms in Eq. (44) containing $\int_{x_n}^{x_{n+1}} e(x)\,dx$ are $O(h^9)$. So unless h is large, contribution of these terms to the RCMS local error is negligible. Thus, to see the effect of the leading term in Eq. (44) very large h steps must be taken. This is illustrated in Figs. 6 and 7.

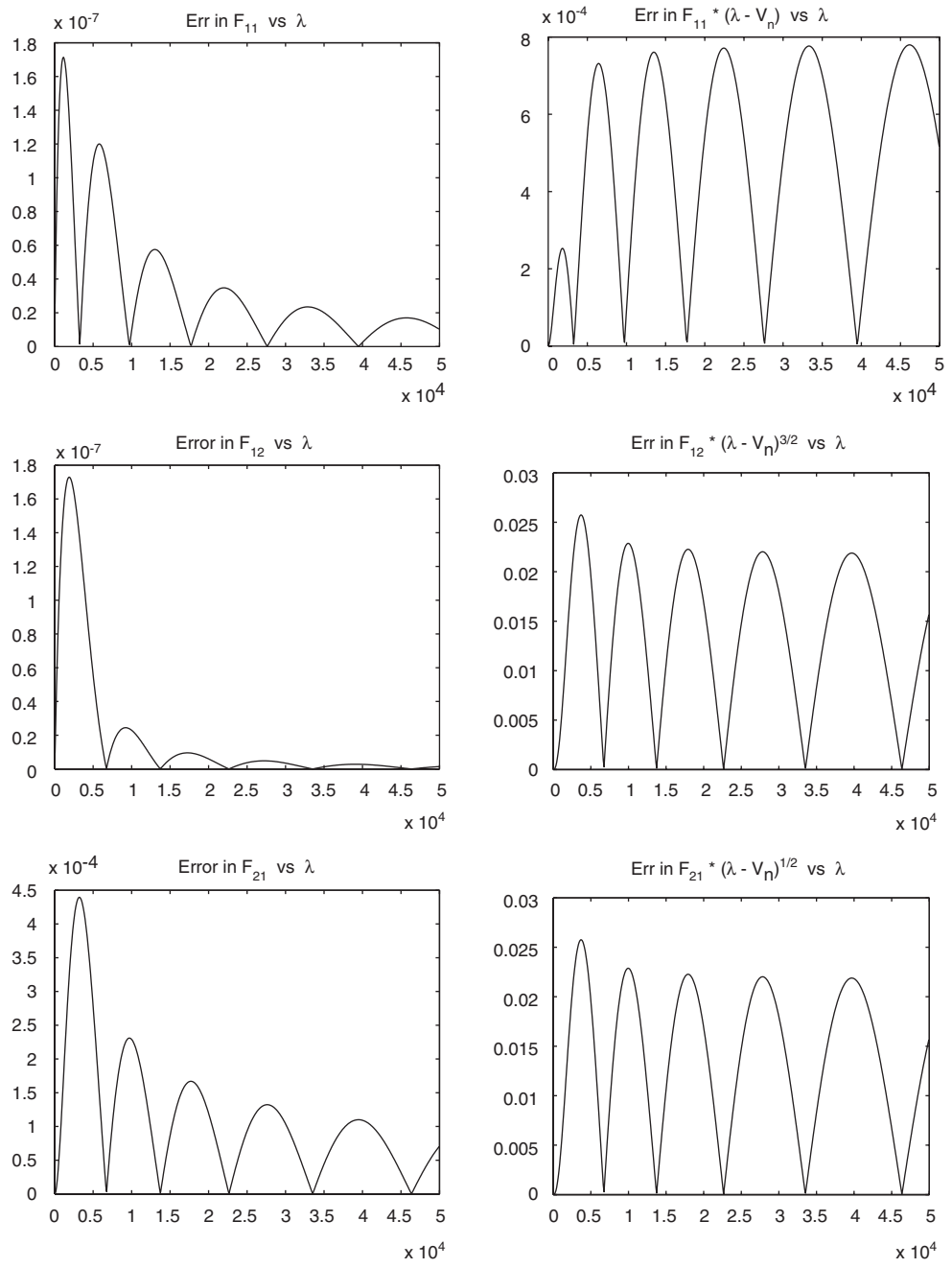

Fig. 6. One-dimensional Schrödinger, RCMS error is independent of, or decays with, increasing λ.

Entries of local error, in approximation of the fundamental solution vs λ, for $h = 0.1$, $V(x) = (\sin(4\pi x) + \cos(4\pi x)) \exp(-x) \exp(3\cos(x))$, $x \in [0, 0.1]$. The contribution of terms with $\int e(x)$ to the local error is negligible and the next order terms in (44) dominate. In the right column $e_{i,j}$ is multiplied by $(\lambda - V_n)^{r/2}$, r being given by the higher order terms in Eq. (44).

5. The benefits of averaging—integrators with exact asymptotics

Our discussion repeatedly invokes constant approximations of functions obtained by averaging. Thus in the Schrödinger equation $V_n = 1/(x_{n+1} - x_n)$ Gauss-quad ($\int_{x_n}^{x_{n+1}} V(x)\,\mathrm{d}x$) was the constant approximation of $V(x)$, and in type A

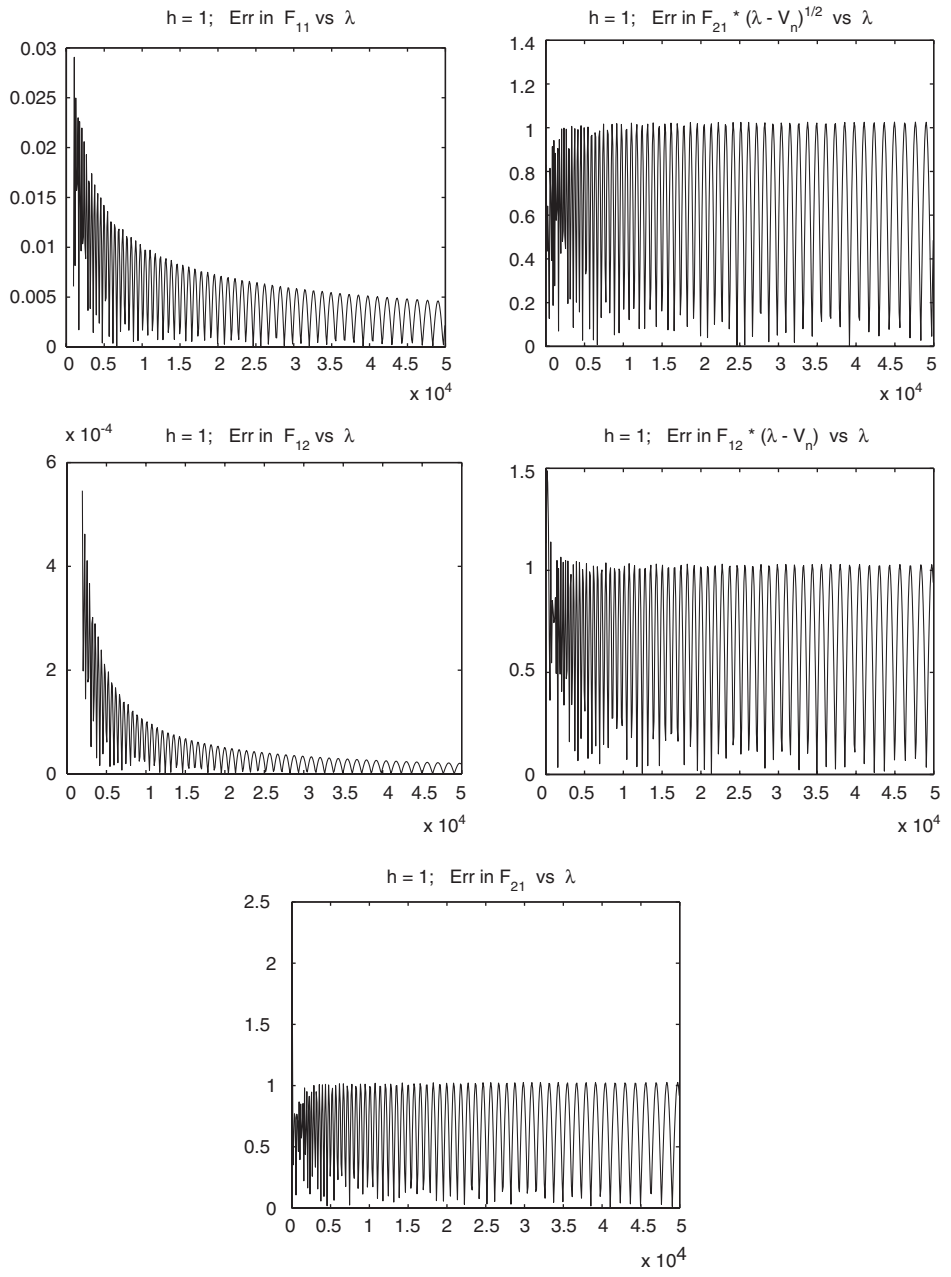

Fig. 7. One-dimensional Schrödinger, RCMS error is independent of, or decays with, increasing λ.

Local error in approximation of the fundamental solution vs λ for $h = 1$, $V(x) = (\sin(4\pi x) + \cos(4\pi x)) \exp(-x) \exp(3\cos(x))$, $x \in [0, 1]$. The large h step is chosen to enhance the contribution of terms with $\int e(x)$ to the error. In the right column $e_{i,j}$ is multiplied by $(\lambda - V_n)^{r/2}$, r being given by the leading order terms in Eq. (44). Note that where they appear, the large errors are due to the large step size h.

equations $A_1(t)$ was similiarly approximated by $\bar{A}_1$. It turns out that such averaging approximations have important implications.

First, recall that Qf is the interpolation polynomial equal to f on the Legendre points, which are the quadrature nodes for obtaining V_n. It has already been noted that

$$\text{if} \quad p(x) = Q(V(x) - V_n) \quad \text{then} \quad \int_{x_n}^{x_{n+1}} p(x)\,\mathrm{d}x = 0. \tag{49}$$

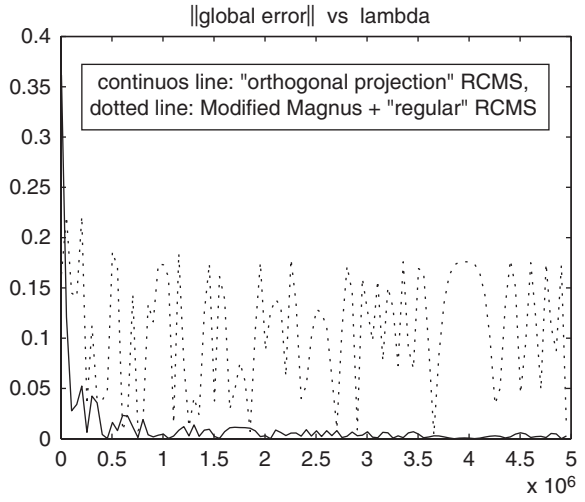

Fig. 8. Orthogonal projection RCMS converges to exact asymptotic solution.

The Coffey–Evans equation from Fig. 4 was integrated with increasing values of λ. The norm of the error in approximation of the fundamental solution, $\|y(\lambda, 0, 1) - \bar{y}(y, 0, 1)\|$, is plotted versus λ for orthogonal projection RCMS (continuous line), Filon–Legendre RCMS, and modified Magnus (indistinguishable results, dotted line) all fourth order. As predicted by our analysis the error envelope of orthogonal projection RCMS decays to zero as $O(1/\sqrt{\lambda})$, while the error envelopes of "regular" Filon–Legendre RCMS and of modified Magnus are constant. For each value of λ the step sizes used to generate the approximation $\bar{y}$, and the "exact" solution y, were $h = \frac{1}{2}$, and $h = \frac{1}{8000}$, respectively.

This property leads to cancellations and simplifications (considerable, but not drastic) in the calculation of right correction Magnus series elements. To see this consider integration by parts of (51), (52). The same simplifications occur in the Frenet–Serret case.

Second, our surprising Theorem 2, backed by numerical results, shows that the RCMS integrator applied here to the 1D Schrödinger equation is eighth order using the first two Magnus terms. Eq. (49) is a crucial ingredient in the proof, given in [6]. The linear oscillators discussed in [9] can be viewed as 1D Schrödinger equations with $V(x) = -g(x)$ and $\lambda = 0$. In [9] it is shown that the Modified Magnus method using the first two Magnus terms with $V_n = V((x_{n+1} + x_n)/2)$ and with exact integrations is only seventh order, giving rise to the suspicion that the higher order predicted by Theorem 2 is a result of the averaging approximation V_n. This (possible) benefit of averaging approximants is particular to the 1D Schrödinger equation and was not observed in the Frenet–Serret case.

Third, the discussion leading to Eq. (46), giving the asymptotic solution of the 1D Schrödinger equation, shows that averaging approximations are an important analytic tool. Generally, given the ODE (2) to obtain the asymptotics of the exact solution as $\lambda \to \infty$ we have expanded exact right corrections in a series $u_n = \sum_{j=0}^{\infty} (1/q^j) g_j$ (in our examples $q \sim \lambda^r$, $r > 0$). Choosing $\bar{A}_1 = (1/(t_{n+1} - t_n)) \int_{t_n}^{t_{n+1}} A_1(t)\, dt$ exactly, gives $g_0 = 0$ which shows that for $t \in [t_n, t_{n+1}]$ the asymptotic fundamental solution of (2) is $\lim_{\lambda\to\infty} y = \exp[(t - t_n)(\lambda A + \bar{A}_1)]$. Note that this argument does not require $[t_n, t_{n+1}]$ to be a small interval. The asymptotic form of the exact solution determines error propagation, as shown in (20) and [9]. The fact that its form is "built in" our analysis is (partly) a consequence of considering averaging approximations $\bar{A}_1$.

Fourth, let $\prod_m$ be the orthogonal projection operator, with respect to the inner product $\langle f|g\rangle = \int_{x_n}^{x_{n+1}} f(x)g(x)\, dx$, onto the space of degree m polynomials. Suppose we take $V_n = (1/(x_{n+1} - x_n)) \int_{x_n}^{x_{n+1}} V(x)\, dx$ exactly, together with $p(x) = \prod_m (V(x) - V_n)$. The discussion after Lemma 1 shows that to construct a fourth order RCMS integrator for the 1D Schrödinger equation with this choice of V_n, $p(x)$, we need the first Magnus term with linear polynomials $m = 1$. It can be shown that (47) gives the leading terms in the asymptotic expansion of the global error of such an integrator. Our choice of V_n, $p(x)$ gives $M_{n-k} = N_{n-k} = 0$ and so the leading term of the global error is $O(1/\sqrt{\lambda})$, i.e. the approximations generated by such an "orthogonal projection" RCMS integrator will converge to the exact solution as λ grows! In contrast, the error envelope of "usual" Filon–Legendre RCMS (with degree m interpolating polynomials on the Legendre points) described in the previous parts of this work, or of (Filon–Legendre) modified Magnus, will be a constant equal to $m + 1$ point Gaussian quadrature error which is $O(h^{2m+3})$. These predictions are supported by

Fig. 8 where the error of "orthogonal projection" RCMS is compared to those of "Filon–Legendre" RCMS and modified Magnus, all fourth order integrators, applied to the Coffey–Evans problem with increasing λ. Higher order "orthogonal projection" RCMS and "orthogonal projection" right correction Neumann integrators are of course also possible. The form of RCMS local error for Frenet–Serret (28) shows that "orthogonal projection" RCMS will also exhibit exact asymptotics in this case.

Calculating orthogonal projection of functions requires analytic integration of inner products. The construction of general purpose numerical ODE software based on exact quadratures seems rather hard (although not necessarily impossible in the era of symbolic computation). However, when a specific problem is at hand and accurate answers are required for large parameter values "orthogonal projection" RCMS may be useful.

6. Conclusion

Our work discusses efficient numerical integration of oscillatory linear ODEs of form (1), which are perturbations of constant coefficient ODEs. Two essential steps are taken, transformation to the right correction equation and application of an integral series representation of the solution of this equation. We name this RCIS, the Right Correction Integral Series approach. RCMS, the modified Magnus method from [9], the integrator for the 1D Schrödinger equation from [15] and the integrators for near adiabatic quantum mechanical propagation from [17,18], are examples of RCIS schemes. The first two use the Magnus series and the others use the Neumann series to integrate the right correction equation. Their exceptional performance illustrates the power of the RCIS approach.

We emphasize the degrees of freedom inherent in this approach; the integral series representing the right correction, the constant approximations $\bar{A}_1$, and the method of obtaining polynomial approximants of $A_1(t) - \bar{A}_1$ (which defines the quadrature method), all can be chosen in various ways giving integrators suitable for highly oscillatory problems but with different properties.

Two examples involving matrices with purely imaginary or zero eigenvalues were studied in detail here. These are the 1D Schrödinger and the type A equations. The important aspects of quadrature (see also [10,13]) and error analysis were developed for RCMS and can be used for other RCIS schemes. The importance of constant approximations $\bar{A}_1$ calculated by averaging of $\overline{A_1(t)}$ was noted. It was shown that they determine the exact asymptotic form of solutions, and that together with polynomial approximants of $A_1(t) - \bar{A}_1$ obtained by orthogonal projection RCMS integrators with exact asymptotics are constructed.

Several important points call for further research. Our brief remark on the case $\lambda < V(x)$ in the 1D Schrödinger equation shows that the RCIS approach may also perform well when the involved matrices have eigenvalues with nonzero real part. Application of RCMS for such problems may be explored.

In this work the perturbation, $A_1(t)$, was assumed not to vary much on the scale of solution oscillations. This was used to approximate $A_1(t)$ by polynomials, on intervals large with respect to the scale of solution oscillation. Thus analytical integration was possible in the Magnus series (Neumann series in [15]) of the right correction equation. The crucial point here is analytic integration over large intervals *not* polynomial approximation. If $A_1(t)$ is highly oscillatory it may be expanded in a Fourier series. Analytical integration in an integral series representation of the right correction will still be possible. In this way efficient, long step, integrators may be constructed for more general perturbations $A_1(t)$.

The Neumann series (5) can have great value in numerical analysis. Like other integral series representations of ODE solutions it is extremely suitable for ODEs with highly oscillatory coefficient matrix. In [7] we observed that since the Neumann series does not use the matrix exponential, or other computationally costly transformations, it may be used for right correction integrators applied to large systems of equations. This line of work was recently taken in [11].

The possibility of even faster error decay with increasing λ should be explored. This may be achieved if jets (the vector of higher derivatives at a point) of the entries of $A_1(t) - \bar{A}_1$ at interval endpoints are used in the formulas giving $\bar{\sigma}$, instead of jets of the entries of the polynomial approximation $P(t) \approx A_1(t) - \bar{A}_1$. This suggestion leads to RCMS (RCIS) integrators which are based on asymptotic expansion of the terms in the right correction Magnus series (other series). Particularly intriguing is the possibility of RCMS integrators with exact *accelerated* asymptotics. These may be obtained by a refined choice of $P(t)$ combining the requirement $\int_{t_n}^{t_{n+1}} P(t) - (A_1(t) - \bar{A}_1)\,\mathrm{d}t = 0$ with requirements on equality of the jets of $P(t)$, $(A_1(t) - \bar{A}_1)$ at interval endpoints. The purpose is to nullify as many terms as possible in the head of the asymptotic error expansion leaving a remainder that rapidly decays with increasing λ.

Another direction is treatment of highly oscillatory linear ODEs which are perturbations of analytically solvable (non-constant coefficient) ODEs. Yet another is extension of the RCIS approach to non-linear equations, a preliminary discussion of which is given in [9].

Acknowledgements

We are indebted to Arieh Iserles and the anonymous referees for valuable comments, and to Yoseph Yomdin and David Tannor for their support and encouragement. The work of J. S. was supported in part by The Israel Science Foundation.

Appendix A. Formulas for approximation of Magnus series

A.1. One-dimensional Schrödinger equations

A_{ij}, the entries in the first Magnus series term, are obtained using repeated integration by parts in $\int_0^h [B(x)]_{ij}\,\mathrm{d}x$, where $B(x)$ is the matrix in the right correction equation (41). $p(x)$ appearing here is a cubic polynomial approximation of $V(x) - V_n$ on a given grid interval. It is obtained by Lagrangian interpolation from the four Legendre points in $[x_n, x_{n+1}]$. The calculations here are done for the interval $[0, h]$ but they apply to any grid interval via a simple coordinate translation. We write q for q_n.

$$\begin{aligned} A_{11} = -A_{22} = &-\frac{1}{4q^2}(p(0) - \cos(2hq)p(h)) - \frac{1}{8q^3}\sin(2hq)p'(h) + \frac{1}{16q^4}(p''(0) \\ &- \cos(2hq)p''(h)) + \frac{1}{32q^5}\sin(2hq)p'''(0), \end{aligned}$$

$$\begin{aligned} A_{21} = q^2 A_{12} = &\frac{1}{4q}\sin(2hq)p(h) - \frac{1}{8q^2}(p'(0) - \cos(2hq)p'(h)) - \frac{1}{16q^3}\sin(2hq)p''(h) \\ &+ p'''(0)\frac{1}{32q^4}(1 - \cos(2hq)). \end{aligned}$$

The second Magnus series term is $\int_0^h [\int_0^x B(y)\,\mathrm{d}y, B(x)]\,\mathrm{d}x$. Performing the commutation, the following integrals appear:

$$I = \int_0^h \left(\int_0^x p(y)\cos(2yq)\,\mathrm{d}y\right) p(x)\sin(2xq)\,\mathrm{d}x, \tag{50}$$

$$I_1 = 2\int_0^h \left(\int_0^x p(y)\,\mathrm{d}y\right) p(x)\sin(2xq)\,\mathrm{d}x, \tag{51}$$

$$I_2 = \int_0^h \left(\int_0^x p(y)\,\mathrm{d}y\right) p(x)\cos(2xq)\,\mathrm{d}x. \tag{52}$$

Integrating by parts and rearranging we obtain

$$\begin{aligned} I = \frac{1}{q}\Bigg(\Bigg(\Bigg(\Bigg(\Bigg(\Bigg(\Bigg(hp'''(0)^2\frac{1}{1008} - p'''(0)p''(h)\frac{1}{144}\Bigg)h + \frac{1}{60}p'''(0)p'(h) + \frac{1}{80}p''(h)^2\Bigg)h \\ -\frac{1}{48}p'''(0)p(h) + \frac{5}{80}p'(h)p''(h)\Bigg)h\Bigg) \\ +\frac{1}{12}(p'(h)^2 + p(h)p''(h))\Bigg)h - \frac{1}{4}p(h)p'(h)\Bigg)h + \frac{1}{4}p(h)^2\Bigg)h \\ + \frac{h^4}{4}\left(\frac{1}{2}p''(0) + \frac{p'''(0)}{2}h\right)\left(p'(0) + h\left(2\frac{1}{2}p''(0) + \frac{p'''(0)}{2}h\right)\right) \end{aligned}$$

$$
\begin{aligned}
&- \frac{1}{q^2}\frac{1}{16}\sin(4hq)p(h)^2\\
&+ \frac{1}{q^3}\left(\left(\left(\left(\left(-\frac{1}{80}p'''(0)^2h + \frac{1}{96}p'''(0)p''(h)\right)h - \frac{1}{48}p'''(0)p'(h) - \frac{1}{96}p''(h)^2\right)h\right.\right.\right.\\
&\left.\left.\left.+\frac{1}{32}p'''(0)p(h) + \frac{1}{32}p'(h)p''(h)\right)h - \frac{1}{16}p(h)p''(h)\right)h - \frac{1}{16}p(0)p'(0)\right.\\
&\left.+\frac{1}{8}\cos(2hq)p(h)p'(0) - \frac{1}{16}\cos(4hq)p(h)p'(h)\right)\\
&+ \frac{1}{q^4}\left(-\frac{1}{16}\sin(2hq)p'(0)p'(h) + \sin(4hq)\left(\frac{1}{64}p'(h)^2 + \frac{1}{32}p(h)p''(h)\right)\right)\\
&+ \frac{1}{q^5}\left(\frac{1}{64}p'''(0)p(0) + \frac{1}{64}p'(0)p''(0) - \cos(2hq)\left(\frac{1}{32}p'''(0)p(h) - \frac{1}{32}p'(0)p''(h)\right.\right.\\
&\left.\left.+p'(0)\left(\frac{1}{2}p''(0) + \frac{p'''(0)}{2}h\right)\right)\right.\\
&\left.+\cos(4hq)\left(\frac{1}{64}p'''(0)p(h) + \frac{1}{64}p'(h)p''(h)\right)\right)\\
&+ \frac{1}{128q^6}\sin(2hq)(2p'''(0)(p'(0)+p'(h)) - \cos(2hq)(2p'''(0)p'(h) + p''(h)^2))\\
&- \frac{1}{256q^7}p'''(0)(p''(0) + (-2\cos(2hq) + \cos(4hq))p''(h))\\
&+ \frac{1}{1024q^8}p'''(0)^2(-4\sin(2hq) + \sin(4hq)),
\end{aligned}
$$

$$
\begin{aligned}
I_1 = {} & \sin(2hq)K_2 + \cos(2hq)K_1 + \frac{1}{4q^2}\left(p(0) + h\left(p'(0) + h\left(\frac{1}{2}p''(0) + \frac{p'''(0)}{6}h\right)\right)\right)^2\sin(2hq)\\
&- \frac{3}{4q^3}p(0)p'(0) + \frac{5}{8q^5}\left(p'(0)p''(0) + \tfrac{1}{2}p'''(0)p(0)\right) - \frac{35}{64q^7}p'''(0)p''(0) - \frac{35}{64q^8}p'''(0)^2\sin(2hq),
\end{aligned}
$$

$$
\begin{aligned}
I_2 = {} & \sin(2hq)\frac{K_1}{2} - \frac{\cos(2hq)}{2}\left(K_2 + \frac{1}{4q^2}p(h)^2\right) + \frac{1}{4q^2}p(0)^2\\
&- \frac{1}{2q^4}\left(\frac{3}{8}p'(0)^2 + \tfrac{1}{2}p(0)p''(0)\right) + \frac{1}{64q^6}\left(15(p'''(0)p'(0) + 10p''(0)^2)\right)\\
&- \frac{35}{128q^8}p'''(0)^2(\tfrac{1}{2} - \cos(2hq)),
\end{aligned}
$$

where

$$
K_1 = \frac{3}{4q^3}p(h)p'(h) - \frac{5}{8q^5}(p'(h)p''(h) + \frac{1}{2}p'''(0)p(h)) + \frac{35}{64q^7}p'''(0)p''(h),
$$

$$
\begin{aligned}
K_2 = {} & \frac{1}{4q^2}p(h)^2 - \frac{1}{2q^4}\left(\frac{3}{4}p'(h)^2 + p(h)p''(h)\right)\\
&+ \frac{5}{16q^6}\left(p''(h)^2 + \frac{3}{2}p'''(0)p'(h)\right) + \frac{35}{128q^8}p'''(0)^2.
\end{aligned}
$$

The right correction equation Magnus series truncated after the first two terms is approximated by

$$\bar{\sigma} = \begin{pmatrix} A_{11} & A_{12} \\ A_{21} & A_{22} \end{pmatrix} - \frac{1}{2} \begin{pmatrix} \dfrac{I_2}{q^2} & -\dfrac{I_1}{q^3} + \dfrac{I_2}{q^4} \\ 2A_{21}A_{22} - \dfrac{I}{q} - \dfrac{I_1}{2q} & -\dfrac{I_2}{q^2} \end{pmatrix}.$$

A.2. Perturbed constant coefficient Frenet–Serret equations

The matrix $B(t)$ in the transformed right correction equation for the perturbed constant coefficient Frenet–Serret equations is given in (25). We write q for $\tilde{\lambda}$. The functions f_1 and f_2 appearing here are the quadratic polynomials approximating f_1 and f_2 from (25). Thus

$$f_1(t) = d_1 + c_1 t + b_1 t^2,$$
$$f_2(t) = d_2 + c_2 t + b_2 t^2.$$

We define $Z(t) = f_2(t) \int_0^t f_1(s)\,\mathrm{d}s$. The six coefficients $d_1, c_1, b_1, d_2, c_2, b_2$ determine all the evaluations of f_1, f_2, Z and their derivatives appearing below.

The first Magnus series term is $\int_0^h B(t)\,\mathrm{d}t$. Integration by parts gives

$$A_{21} = d_1 h + \frac{1}{2} c_1 h^2 + \frac{1}{3} b_1 h^3,$$

$$A_{13} = \frac{1}{q}\sin(hq) f_2(h) + \frac{1}{q^2}(\cos(hq) f_2''(h) - f_2''(0)) - \frac{1}{q^3}\sin(hq) f_2''(h),$$

$$A_{32} = -\frac{1}{q}(\cos(hq) f_2''(h) - f_2''(0)) + \frac{1}{q^2}\sin(hq) f_2''(h) + \frac{1}{q^3}(\cos(hq) f_2''(h) - f_2''(0)).$$

The second Magnus series term is $\int_0^h [\int_0^t B(x)\,\mathrm{d}x, B(t)]\,\mathrm{d}t$. Performing the commutation, the following integrals appear:

$$I = \int_0^h \left(\int_0^x f_2(y)\cos(2yq)\,\mathrm{d}y \right) f_2(x)\sin(2xq)\,\mathrm{d}x,$$

$$I_1 = \int_0^h Z(t)\sin(2tq)\,\mathrm{d}t,$$

$$I_2 = \int_0^h Z(t)\cos(2tq)\,\mathrm{d}t.$$

Note that if f_2 is replaced by p, I is identical to the expression with the same name appearing in the RCMS formulas for the 1D Schrödinger equation. Moreover, if f_1 is also replaced by p then I_1 and I_2 here transform to those appearing in the discussion on the 1D Schrödinger equation.

The formulas for I used here are obtained from those in the 1D Schrödinger equation by replacing any appearance of $f_2''' \sim p'''$ by 0. I_1 and I_2 are obtained by a simple integration by parts

$$\begin{aligned} I_1 = &-\frac{1}{q}(\cos(hq)Z(h) - Z(0)) + \frac{1}{q^2}\sin(hq)Z'(h) + \frac{1}{q^3}(\cos(hq)Z''(h) - Z''(0)) \\ &- \frac{1}{q^4}\sin(hq)Z'''(h) - \frac{1}{q^5}(\cos(hq)Z^{(4)}(h) - Z^{(4)}(0)) + \frac{1}{q^6}\sin(hq)Z^{(5)}(h), \end{aligned}$$

$$\begin{aligned} I_2 = &\frac{1}{q}\sin(hq)Z(h) + \frac{1}{q^2}(\cos(hq)Z'(h) - Z'(0)) - \frac{1}{q^3}\sin(hq)Z''(h) \\ &- \frac{1}{q^4}(\cos(hq)Z'''(h) - Z'''(0)) + \frac{1}{q^5}\sin(hq)Z^{(4)}(h) + \frac{1}{q^6}(\cos(hq)Z^{(5)}(h) - Z^{(5)}(0)). \end{aligned}$$

Now $\bar{\sigma}$ the RCMS approximation of the Magnus series can be written as

$$\bar{\sigma} = \begin{pmatrix} 0 & -A_{21} & A_{13} \\ A_{21} & 0 & -A_{32} \\ -A_{13} & A_{32} & 0 \end{pmatrix} - \frac{1}{2} \begin{pmatrix} 0 & 2I - A_{13}A_{32} & 2I_1 - A_{21}A_{32} \\ A_{13}A_{32} - 2I & 0 & 2I_2 - A_{21}A_{13} \\ A_{21}A_{32} - 2I_1 & A_{21}A_{13} - 2I_2 & 0 \end{pmatrix}.$$

References

[1] N.D. Aparicio, S.J.A. Malham, M. Oliver, Numerical evaluation of the Evans function by Magnus Integration, preprint, 2003.
[2] L. Carmel, A. Mann, Geometrical approach to two level Hamiltonians, Phys. Rev. A 61 (2000) 052113.
[3] P.J. Davis, P. Rabinowitz, Methods of Numerical Integration, second ed., Academic Press, New York, 1984.
[4] I. Degani, Lie group numerical integrators and linear differential equations depending on a large parameter, Ph.D. research proposal (advisors: J. Schiff, Y. Yomdin), Feinberg Graduate School, Weizmann Institute of Science, 2000 (submitted 11/12/2000).
[5] I. Degani, Lie group numerical integrators and linear differential equations depending on a large parameter, Ph.D. interim report (advisors: J. Schiff, Y. Yomdin), Feinberg Graduate School, Weizmann Institute of Science, 2002 (submitted 14/3/2002).
[6] I. Degani, RCMS—Right Correction Magnus Schemes for oscillatory ODEs and cubature formulae and commuting extensions, Ph.D. Thesis (advisors: J. Schiff, Y. Yomdin), Feinberg Graduate School, Weizmann Institute of Science, 2004 (submitted 12/8/04).
[7] I. Degani, J. Schiff, RCMS: Right Correction Magnus Series approach for integration of linear ordinary differential equations with highly oscillatory solution, Technical Report MCS03-04, Weizmann Institute of Science, Department of Computer Science and Applied Mathematics, 2003.
[8] T. Håvie, Remarks on an expansion for integrals of rapidly oscillating functions, BIT 13 (1973) 16–29.
[9] A. Iserles, On the global error of discretization methods for highly-oscilatory ordinary differential equations, BIT 42 (2002) 561–599 see also Technical Report 2000/N A11, DAMTP University of Cambridge; and Think globally act locally: solving highly-oscillatory ordinary differential equations, Appl. Numer. Math. 43 (2002) 145–160.
[10] A. Iserles, On the numerical quadrature of highly oscillating integrals I: Fourier transforms, Technical Report NA2003/05, DAMTP University of Cambridge, 2003.
[11] A. Iserles, On the method of Neumann series for highly oscillatory equations, Technical Report NA2004/02, DAMTP University of Cambridge, 2004.
[12] A. Iserles, S.P. Nørsett, On the solution of linear differential equations on Lie groups, Philos. Trans. Roy. Soc. A 357 (1999) 983–1020.
[13] A. Iserles, S.P. Nørsett, Efficient quadrature of highly oscillatory integrals using derivatives, Technical Report NA2004/03, DAMTP University of Cambridge; see also On quadrature methods for highly oscillatory integrals and their implementation, Technical Report NA2004/05, DAMTP University of Cambridge, 2004.
[14] A. Iserles, H. Munthe-Kass, S.P. Nørsett, A. Zanna, Lie group methods, Acta Numerica 2000 (2000) 215–365.
[15] L.Gr. Ixaru, H. De Meyer, G. Vanden Berghe, CP methods for the Schrödinger equation revisited, J. Comput. Appl. Math. 88 (1997) 289–314.
[16] L.Gr. Ixaru, H. De Meyer, G. Vanden Berghe, SLCPM12—A program for solving regular Sturm–Liouville problems, Comput. Phys. Comm. 118 (1999) 259–277.
[17] T. Jahnke, Long time step integrators for almost adiabatic quantum dynamics, SIAM J. Sci. Comput. 25 (2004) 2145–2164 (preprints released in 2002).
[18] T. Jahnke, C. Lubich, Numerical integrators for quantum dynamics close to the adiabatic limit, Numer. Math. 94 (2003) 289–314.
[19] Y. Kats, D.A. Kessler, Y. Rabin, Frenet algorithm for simulations of fluctuating continous elastic filaments, Phys. Rev. E 65 (2002) 020801R.
[20] P.C. Moan, Efficient approximation of Sturm–Liouville problems using Lie group methods, Technical Report 1998/NA11, DAMTP University of Cambridge, 1998.
[21] S. Pruess, Estimating the eigenvalues of Sturm–Liouville problems by approximating the differential equation, SIAM J. Numer. Anal. 10 (1973) 55–68.
[22] S. Pruess, C.T. Fulton, Mathematical software for Sturm–Liouville problems, ACM Trans. Math. Software 19 (1993) 360–376.
[23] J.D. Pryce, Numerical Solution of Sturm–Liouville Problems, Clarendon Press, Oxford, 1993.
[24] A. Ralston, P. Rabinowitz, A First Course in Numerical Analysis, second ed., Dover, New York, 2001.
[25] J. Schiff, S. Shnider, A natural approach to the numerical integration of Riccati differential equations, SIAM J. Numer. Anal. 36 (1999) 1392–1413.
[26] M. Spivak, A Comprehensive Introduction to Differential Geometry, vol. 2, Publish or Perish, 1979.
[27] D.J. Tannor, Introduction to Quantum Mechanics: A Time Dependent Perspective, University Science Press, Sausalito, 2001.